

Loop diagrams in the kinetic theory of waves

Vladimir Rosenhaus¹, Daniel Schubring¹, Md Shaikot Jahan Shuvo¹, and Michael Smolkin²

¹ *Initiative for the Theoretical Sciences
The Graduate Center, CUNY
365 Fifth Ave, New York, NY 10016, USA*

² *The Racah Institute of Physics
The Hebrew University of Jerusalem
Jerusalem 91904, Israel*

Recent work has given a systematic way for studying the kinetics of classical weakly interacting waves beyond leading order, having analogies with renormalization in quantum field theory. An important context is weak wave turbulence, occurring for waves which are small in magnitude and weakly interacting, such as those on the surface of the ocean. Here we continue the work of perturbatively computing correlation functions and the kinetic equation in this far-from-equilibrium state. In particular, we obtain the next-to-leading-order kinetic equation for waves with a cubic interaction. Our main result is a simple graphical prescription for the terms in the kinetic equation, at any order in the nonlinearity.

Contents

1. Introduction	1
2. Interacting waves	2
3. Loops	6
3.1. Quartic interaction	6
3.2. Cubic interaction	8
3.3. Next-to-leading order kinetic equation for cubic interactions	11
4. Prescription for a general Feynman diagram	13
5. Discussion	17
A. Perturbative Liouville equation for waves	18
B. Symmetries	23
C. Manipulating the kinetic equation	28
D. Contact terms and lollipop diagrams	31

1. Introduction

Kinetic equations are widely used to study equilibrium and non-equilibrium dynamics, transport, and even turbulence. The kinetic equations are a truncation of a vast hierarchy, involving multimode correlators. An important problem is understanding when this truncation is correct. It has long been recognized in the context of particles (the Boltzmann equation) that corrections can be large and give qualitatively new effects [1–4], and have been studied in a number of works [5–11]. The kinetics of waves [12] is particularly fascinating as it allows for the study of weak wave turbulence [13], an old subject [14] undergoing a recent experimentally driven revival in a range of physical contexts, see e.g. [15] and references therein, going beyond the canonical example of ocean waves [16,17]. For waves, unlike for particles, there hasn't been a systematic study of higher order corrections to the leading order kinetic equations.

The connection between kinetic equations and quantum field theory [18] has given an effective way of computing corrections, and made it evident that they are important, modifying the standard assumptions on the range of applicability of wave turbulence [19]. In short, even if the coefficients of the nonlinear terms in the Hamiltonian are numerically small, intermediate states in the scattering

of waves (loop diagrams) can have interacting waves with vastly different momenta. This large ratio of momenta can then overpower the smallness of the interaction coefficient, making higher order loop diagrams seemingly dominant rather than suppressed. Summing an infinite class of loop diagrams may then give a new, renormalized, kinetic equation, which encodes phenomenon not captured by the standard leading order kinetic equation [19]. The need to compute loop diagrams, in a simple and compact way, and potentially to high orders, is acute. This is what we seek to address, extending our previous work [18, 20]. Our discussion will be confined to classical kinetic theory (although we study it using tools of quantum field theory); the extension to quantum kinetic theory will be discussed in [21] and is relevant for studies of thermalization and wave turbulence in QCD, see e.g. [22–26].

In Sec. 2 we review the context of interacting waves and the leading order in nonlinearity (tree-level) correlation functions and the corresponding kinetic equation. In Sec. 3 we compute the one-loop correction to the correlation functions. We do this for a theory with a cubic or quartic interaction. In Sec. 3.3 we use this to give the next-to-leading order kinetic equation for a theory with a cubic interaction. This extends the results of [18, 20] which studied the simplest case, of a quartic interaction. In Sec. 4 we give our main result: a prescription for almost immediately writing down the contribution of any Feynman diagram, at any order in the coupling, to an equal time correlation function. This turns the problem of finding higher order terms in the kinetic equation into a simple bookkeeping exercise. We conclude in Sec. 5.

In Appendix A we show that an alternate method for deriving the higher order terms in the kinetic equation, by perturbatively solving the Liouville equation and performing a phase space average [20], exactly reproduces – at each order in perturbation theory – the method used in the main body, of averaging over external Gaussian random forcing which is set to zero at the end. In Appendix B we discuss symmetries of the Hamiltonian and how it relates different terms in the kinetic equation, which is discussed further in Appendix C. A few technical remarks are relegated to Appendix D.

2. Interacting waves

Our context will be that of classical interacting waves. This occurs in many situations, ranging from surface gravity waves to spin waves. We focus on a single field, which can, for instance, describe the height of the ocean. The variables are the field and its canonical conjugate, though it is often simpler to work with a single complex field a_p , which is the sum of these two. The most general Hamiltonian is a sum of q -body Hamiltonians,

$$H = \sum_{q=2}^{\infty} H_q . \tag{2.1}$$

In particular, H_2 is the free Hamiltonian,

$$H_2 = \sum_p \omega_p a_p^\dagger a_p, \quad (2.2)$$

where a_p^\dagger denotes the complex conjugate of a_p , $a_p^\dagger \equiv a_p^*$. Generally, if one is considering a theory with weak interactions, the higher order the interaction term the more suppressed it is. For this reason, it is common to focus on solely the lowest order nonvanishing term. In general, the first interaction term that dominates is the cubic term, so that the Hamiltonian is truncated to,

$$H = H_2 + H_3 = \sum_p \omega_p a_p^\dagger a_p + \frac{1}{2} \sum_{p_i} \left(\lambda_{p_1 p_2 p_3} a_{p_1}^\dagger a_{p_2} a_{p_3} + \lambda_{p_1 p_2 p_3}^* a_{p_1} a_{p_2}^\dagger a_{p_3}^\dagger \right), \quad (2.3)$$

where for the interaction term there is an implicit momentum conserving delta function $\delta(\vec{p}_1 - \vec{p}_2 - \vec{p}_3)$. In sections that follow, it will be convenient to use the shorthand $\lambda_{123} \equiv \lambda_{p_1 p_2 p_3}$, and similarly for larger q . In some cases the dispersion relation is such that a resonant cubic interaction is forbidden, i.e., it is not possible for the wave to have both $\vec{p}_1 = \vec{p}_2 + \vec{p}_3$ and $\omega_{p_1} = \omega_{p_2} + \omega_{p_3}$. Then the lowest interaction term is quartic. This is the case we focused on in [18] and [20] (the symmetries of the quartic term make it slightly simpler than the cubic term),¹

$$H = H_2 + H_4 = \sum_p \omega_p a_p^\dagger a_p + \sum_{p_1 \dots p_4} \lambda_{p_1 p_2 p_3 p_4} a_{p_1}^\dagger a_{p_2}^\dagger a_{p_3} a_{p_4}. \quad (2.4)$$

In the main body of the text we will focus on the case of $q = 3$ and $q = 4$. The generalization to arbitrary q is straightforward.

Averaging over forcing

Since this is a many-body chaotic system, one has to perform some kind of average in order to have sensible quantities. The averaging that we do here is to add Gaussian-random forcing. In particular, the equations of motion,

$$\dot{a}_k = -i \frac{\partial H}{\partial a_k^\dagger}, \quad (2.5)$$

are modified so as to add forcing, as well as dissipation in order to absorb the flux of energy. The new equations of motion are²,

$$\dot{a}_k = -i \frac{\partial H}{\partial a_k^\dagger} + f_k(t) - \gamma_k a_k, \quad (2.6)$$

¹The cubic couplings have the symmetry $\lambda_{p_1 p_2 p_3} = \lambda_{p_1 p_3 p_2}$ and the quartic couplings have the symmetry $\lambda_{p_1 p_2 p_3 p_4} = \lambda_{p_2 p_1 p_3 p_4} = \lambda_{p_1 p_2 p_4 p_3} = \lambda_{p_3 p_4 p_1 p_2}^*$.

²There are other choices of dissipation one could make, such as $-\frac{\gamma_k}{\omega_k} \frac{\partial H}{\partial a_k^\dagger}$ [27]. In the limit of vanishing dissipation these are all equivalent.

where the forcing is drawn from a Gaussian distribution with variance F_k ,

$$P[f] \sim \exp\left(-\int dt \sum_k \frac{|f_k(t)|^2}{F_k}\right), \quad \langle f_k(t) f_p^*(t') \rangle = F_k \delta(k-p) \delta(t-t'). \quad (2.7)$$

After computing the correlation functions, we take $F_k, \gamma_k \rightarrow 0$ with fixed n_k ,

$$n_k \equiv \frac{F_k}{2\gamma_k}. \quad (2.8)$$

The reason for this notation is that n_k is the occupation number of mode k for the noninteracting theory. Going forward, for notational simplicity, instead of writing F_k , we will write $2\gamma_k n_k$.

It is important to note that we will be computing correlation functions in a stationary state. In other words, we assume that we have a stationary state and then later self-consistently pick F_k and γ_k to ensure this. It will turn out that there are multiple possible stationary states in the zero dissipation limit: the thermal state and the turbulent state. However, nothing in our calculations of the correlation functions and kinetic equation is dependent on the properties of these states; we only need to assume we are computing correlators about a stationary state.

One can compute correlation functions by solving the equations of motion perturbatively in the interaction and then averaging over forcing. For each term in the perturbative expansion one can associate a corresponding Wyld diagram [28, 29].

A more streamlined method for doing this calculation was introduced in [18], and consists of integrating out the forcing at the outset. In particular, our classical stochastic field theory is equivalent to a quantum field theory, with expectation values given by a path integral for a Lagrangian that is the square of the classical, force-free, equations of motion,

$$\langle \mathcal{O}(a) \rangle = \int \mathcal{D}a \mathcal{D}a^\dagger \mathcal{O}(a) e^{-\int dt L}, \quad L = \sum_k \frac{|E_{f=0}|^2}{2\gamma_k n_k}, \quad E_{f=0} = \dot{a}_k + i \frac{\delta H}{\delta a_k^\dagger} + \gamma_k a_k. \quad (2.9)$$

Let us break up the Hamiltonian into the free part, H_2 , and the interacting part, $H_{int} = \sum_{q=3}^\infty H_q$. The Lagrangian is then,

$$L = \sum_k \frac{1}{2\gamma_k n_k} \left| \dot{a}_k + (i\omega_k + \gamma_k) a_k + i \frac{\delta H_{int}}{\delta a_k^\dagger} \right|^2 = L_{free} + L_{int} \quad (2.10)$$

where

$$\begin{aligned} L_{free} &= \sum_k \frac{1}{2\gamma_k n_k} \left| (\partial_t + i\omega_k + \gamma_k) a_k \right|^2 \\ L_{int} &= \sum_k \frac{1}{2\gamma_k n_k} \left[-i(\partial_t + i\omega_k + \gamma_k) a_k \frac{\delta H_{int}}{\delta a_k} + \text{c.c.} \right] + \dots, \end{aligned} \quad (2.11)$$

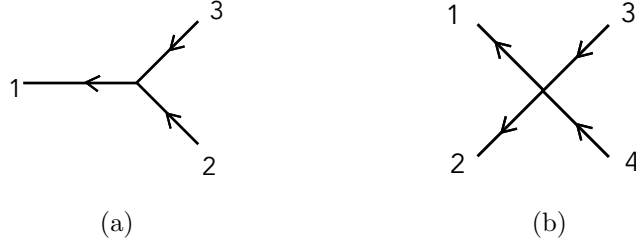


Figure 1: Tree-level Feynman diagrams for (a) cubic (2.15) and (b) quartic interactions (2.16).

where c.c. denotes the complex conjugate. The term contained in the dots of L_{int} that we have left out is the square of the absolute value of $\frac{\delta H_{int}}{\delta a_k}$; we can neglect this term provided that when evaluating Feynman diagrams we drop contact interactions (when two times collide), see Appendix D.

Let us work out the Feynman rules. As usual, the Feynman rules are most convenient in momentum/frequency space. The quadratic term in the Lagrangian, L_{free} , gives the propagator,

$$D_{k,\omega} = n_k \frac{2\gamma_k}{(\omega - \omega_k)^2 + \gamma_k^2} . \quad (2.12)$$

We will use shorthand $D_i \equiv D_{p_i,\omega_i}$, $n_i \equiv n_{p_i}$, and $\gamma_i \equiv \gamma_{p_i}$. Notice that in the limit of $\gamma_k \rightarrow 0$, the propagator becomes a delta function, $n_k 2\pi\delta(\omega - \omega_k)$. It will, however, be important to keep γ_k finite until the very end of the calculation. It will be convenient to define,

$$g_j = \frac{\omega_j - \omega_{p_j} + i\gamma_j}{2\gamma_j n_j i} . \quad (2.13)$$

The Feynman rule for the vertex is³

$$\begin{aligned} \frac{-i}{2} \lambda_{123} (g_1^* - g_2 - g_3) 2\pi\delta(\omega_{1;23}) , & \quad q = 3 , \\ -i \lambda_{1234} (g_1^* + g_2^* - g_3 - g_4) 2\pi\delta(\omega_{12;34}) , & \quad q = 4 , \end{aligned} \quad (2.14)$$

where we have introduced the notation $\omega_{12;3} \equiv \omega_1 + \omega_2 - \omega_3$ and $\omega_{12;34} \equiv \omega_1 + \omega_2 - \omega_3 - \omega_4$. The tree-level frequency space correlation functions are trivially obtained by adding external propagators and accounting for the appropriate combinatorial factors from Wick contractions,

$$\langle a_{p_1,\omega_1} a_{p_2,\omega_2}^\dagger a_{p_3,\omega_3}^\dagger \rangle = -i \lambda_{123} (g_1^* - g_2 - g_3) D_1 D_2 D_3 2\pi\delta(\omega_{1;23}) , \quad q = 3 \quad (2.15)$$

$$\langle a_{p_1,\omega_1} a_{p_2,\omega_2}^\dagger a_{p_3,\omega_3}^\dagger a_{p_4,\omega_4}^\dagger \rangle = -4i \lambda_{1234} (g_1^* + g_2^* - g_3 - g_4) D_1 D_2 D_3 D_4 2\pi\delta(\omega_{12;34}) . \quad q = 4 , \quad (2.16)$$

The corresponding Feynman diagrams are shown in Fig. 1. The time-space correlation functions

³Note that these Feynman rules are not symmetrized.

are Fourier transforms,

$$\langle a_{p_1}(t_1)a_{p_2}^\dagger(t_2)a_{p_3}^\dagger(t_3) \rangle = \int \frac{d\omega_1}{2\pi} \dots \frac{d\omega_3}{2\pi} e^{-i\omega_1 t_1 + i\omega_2 t_2 + i\omega_3 t_3} \langle a_{p_1, \omega_1} a_{p_2, \omega_2}^\dagger a_{p_3, \omega_3}^\dagger \rangle . \quad (2.17)$$

In particular, the equal-time tree-level correlation functions are,

$$\langle a_1 a_2^\dagger a_3^\dagger \rangle = \lambda_{123} \frac{1}{\omega_{p_2, p_3; p_1} + i\epsilon} n_1 n_2 n_3 \left(\frac{1}{n_1} - \frac{1}{n_2} - \frac{1}{n_3} \right) , \quad (2.18)$$

$$\langle a_1 a_2 a_3^\dagger a_4^\dagger \rangle = 4\lambda_{1234} \frac{1}{\omega_{p_3, p_4; p_1, p_2} + i\epsilon} n_1 n_2 n_3 n_4 \left(\frac{1}{n_1} + \frac{1}{n_2} - \frac{1}{n_3} - \frac{1}{n_4} \right) , \quad (2.19)$$

where $\epsilon = \sum_i \gamma_i$ represents the sum over the dissipation constants appearing in the vertex.

An important quantity is the occupation number n_k of mode k , $n_k = \langle a_k^\dagger a_k \rangle$, which is governed by the kinetic equation. Through use of the equations of motion it can be expressed in terms of the equal-time correlation function. In particular, for $q = 3$,

$$\frac{\partial n_k}{\partial t} = \sum_{p_i} (\delta_{kp_1} - \delta_{kp_2} - \delta_{kp_3}) \text{Im} \left(\lambda_{p_1 p_2 p_3} \langle a_{p_1}^\dagger a_{p_2} a_{p_3} \rangle \right) , \quad (2.20)$$

where all operators on the left and the right are evaluated at time t . For the general Hamiltonian (2.1) this has the obvious generalization.

Inserting the tree-level correlation function (2.18) into (2.20) gives the standard kinetic equation for waves [13]. Our goal will be to compute higher order in the coupling corrections to this. In the next section we will therefore turn to computing the equal-time correlation functions perturbatively in the coupling.

3. Loops

The tree-level correlation functions were given in the previous section. Here we will compute their one-loop corrections, first in the case of the quartic interaction and then for the cubic interaction.

3.1. Quartic interaction

The one-loop (order λ^2) correction to the tree-level four-point function for the case of $q = 4$ (quartic interaction) was computed in [18]. One of the corresponding diagrams is shown in Fig. 2; there are two more diagrams with arrows in different directions which we won't discuss here. Here we redo the calculation in a faster way, working in time space instead of frequency space, which is better suited for generalization to higher order loops.

Using the Feynman rules, the contribution of this diagram to the one-loop four-point function,

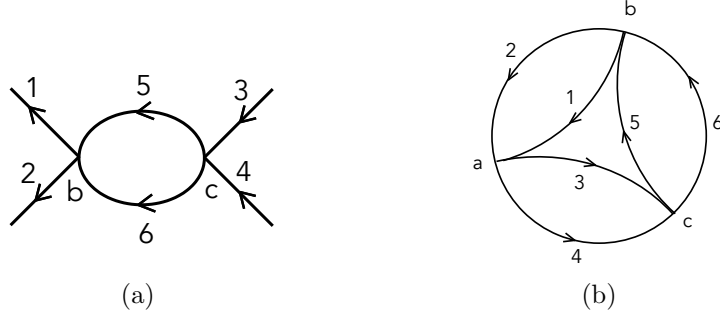


Figure 2: (a) A one-loop diagram contributing to the four-point function. (b) We set the external times to be equal to t_a , represented by the four lines meeting at the point t_a .

with all external times set equal to time t_a , is given by,⁴

$$\langle a_1 a_2 a_3^\dagger a_4^\dagger \rangle(t_a) = 8 \sum_{p_5, p_6} \int \prod_{i=1}^6 \frac{d\omega_i}{2\pi} D_i e^{i\omega_{12;34} t_a} 2\pi\delta(\omega_{12;56}) 2\pi\delta(\omega_{56;34}) V + \dots$$

$$V = -\lambda_{1256} \lambda_{5634} (g_1^* + g_2^* - g_5 - g_6)(g_5^* + g_6^* - g_3 - g_4). \quad (3.1)$$

Writing the frequency delta functions in terms of their Fourier transforms, $2\pi\delta(\omega_{12;56}) = \int dt_b e^{-i\omega_{12;56} t_b}$ and $2\pi\delta(\omega_{56;34}) = \int dt_c e^{-i\omega_{56;34} t_c}$ we get,

$$\langle a_1 a_2 a_3^\dagger a_4^\dagger \rangle(t_a) = 8 \sum_{p_5, p_6} \int \prod_{i=1}^6 \frac{d\omega_i}{2\pi} D_i \int dt_b dt_c e^{i(\omega_1 + \omega_2) t_{ab}} e^{-i(\omega_3 + \omega_4) t_{ac}} e^{-i(\omega_5 + \omega_6) t_{cb}} V + \dots \quad (3.2)$$

We exchange the order of integration, and first evaluate the ω_i integrals. The ω_i integrals are trivial to evaluate, by closing the contour and picking up simple poles. For any particular choice of time orderings of t_a, t_b, t_c , convergence imposes a unique choice of if the contours of integration should be closed in the upper or lower half-plane. In particular, the poles come from the propagators D_i in V . For the integrals $\int \frac{d\omega}{2\pi} e^{-i\omega t_{ij}}$: if $t_{ij} > 0$ then we close in the lower-half plane, picking up the pole $\omega = \omega_p - i\gamma$. If $t_{ij} < 0$ then we close in the upper half plane, picking up the pole $\omega = \omega_p + i\gamma$.⁵

We split the time integrations into $3!$ regions, corresponding to the $3!$ possible time orderings of t_a, t_b, t_c . Unless t_a is the earliest time, one finds a vanishing contribution. This leaves two possible orderings:

Region 1: $t_b > t_c > t_a$

We close the ω_1, ω_2 integrals in the lower half plane, and close the $\omega_3, \omega_4, \omega_5, \omega_6$ integrals in

⁴Our sign convention for the Fourier transform is different here than in the previous section, (2.17), but this doesn't affect the answer.

⁵Notice that we are excluding the possibility of t_b, t_c being equal; see Appendix D.

the upper half plane. The vertex factor V becomes,

$$V = \lambda_{1256} \lambda_{5634} \left(\frac{1}{n_1} + \frac{1}{n_2} - \frac{1}{n_5} - \frac{1}{n_6} \right) \left(\frac{1}{n_3} + \frac{1}{n_4} \right), \quad (3.3)$$

and the time integral becomes,

$$\int_{t_a}^{\infty} dt_c \int_{t_c}^{\infty} dt_b e^{-i(\omega_{p_1} + \omega_{p_2} - 2i\gamma)t_{ba}} e^{i(\omega_{p_3} + \omega_{p_4} + 2i\gamma)t_{ca}} e^{i(\omega_{p_5} + \omega_{p_6} + 2i\gamma)t_{bc}} = \frac{i}{\omega_{p_5, p_6; p_1 p_2} + 4i\gamma} \frac{i}{\omega_{p_3, p_4; p_1, p_2} + 4i\gamma}, \quad (3.4)$$

so that in total we have,

$$8 \sum_{p_5} \lambda_{1256} \lambda_{5634} \prod_i^6 n_i \left(\frac{1}{n_1} + \frac{1}{n_2} - \frac{1}{n_5} - \frac{1}{n_6} \right) \left(\frac{1}{n_3} + \frac{1}{n_4} \right) \frac{i}{\omega_{p_5, p_6; p_1 p_2} + 4i\gamma} \frac{i}{\omega_{p_3, p_4; p_1, p_2} + 4i\gamma}. \quad (3.5)$$

Region 2: $t_c > t_b > t_a$:

We close the $\omega_1, \omega_2, \omega_5, \omega_6$ integrals in the lower half plane, and we close the ω_3, ω_4 integrals in the upper half plane. This vertex factor becomes

$$V = -\lambda_{1256} \lambda_{5634} \left(\frac{1}{n_1} + \frac{1}{n_2} \right) \left(\frac{1}{n_5} + \frac{1}{n_6} - \frac{1}{n_3} - \frac{1}{n_4} \right), \quad (3.6)$$

and the time integral becomes,

$$\int_{t_a}^{\infty} dt_b \int_{t_b}^{\infty} dt_c e^{-i(\omega_{p_1} + \omega_{p_2} - 2i\gamma)t_{ba}} e^{i(\omega_{p_3} + \omega_{p_4} + 2i\gamma)t_{ca}} e^{i(\omega_{p_5} + \omega_{p_6} - 2i\gamma)t_{bc}} = \frac{i}{\omega_{p_3, p_4; p_5, p_6} + 4i\gamma} \frac{i}{\omega_{p_3, p_4; p_1, p_2} + 4i\gamma}, \quad (3.7)$$

so that in total we have,

$$-8 \sum_{p_5} \lambda_{1256} \lambda_{5634} \prod_i^6 n_i \left(\frac{1}{n_1} + \frac{1}{n_2} \right) \left(\frac{1}{n_5} + \frac{1}{n_6} - \frac{1}{n_3} - \frac{1}{n_4} \right) \frac{i}{\omega_{p_3, p_4; p_5, p_6} + 4i\gamma} \frac{i}{\omega_{p_3, p_4; p_1, p_2} + 4i\gamma}. \quad (3.8)$$

The sum of (3.5) and (3.8) reproduces what we found earlier in [18] (see Eq. 4.25 and use the identity A.8 in [20]).⁶

3.2. Cubic interaction

Consider now the equal-time three-point function $\langle a_1 a_2^\dagger a_3^\dagger \rangle(t_a)$ arising from a cubic interaction. The tree-level correlation function, at order λ , was given earlier in (2.18). At order λ^2 all Feynman diagrams vanish. At order λ^3 one has two kinds of diagrams: the ‘‘tetrahedron’’ diagram, which can be viewed as a renormalization of the cubic interaction vertex, and a loop diagram arising

⁶There is an additional Feynman diagram that contributes to the one-loop kinetic equation, whose contribution simply involves transforming the diagram we discussed by $2 \leftrightarrow -3$ and $6 \rightarrow -6$, see [18].

from renormalization of the propagator.

Vertex renormalization: tetrahedron diagram

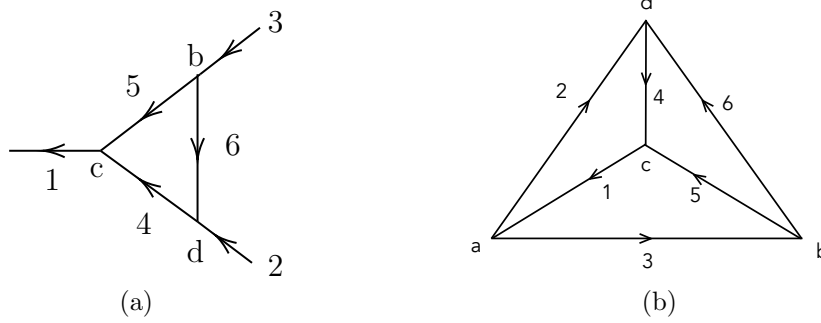


Figure 3: (a) A one-loop diagram contributing to the three-point function. (b) We set the external times to be equal to t_a , represented by the three lines meeting at the point t_a . We refer to this as the tetrahedron diagram

We start with tetrahedron diagram shown in Fig. 3. Evaluating the diagram in an analogous way to the diagram in the previous section, we find its contribution to the equal-time three-point function $\langle a_1 a_2^\dagger a_3^\dagger \rangle$ is equal to,

$$\begin{aligned}
& 2 \sum_{p_4, p_5, p_6} \lambda_{426} \lambda_{356}^* \lambda_{145} \prod_{i=1}^6 n_i \frac{1}{\omega_{p_2, p_3; p_1} + i\epsilon} \\
& \left\{ \frac{1}{n_1} \frac{1}{\omega_{p_2, p_3; p_4, p_5} + i\epsilon} \left[\frac{1}{\omega_{p_3; p_5, p_6} + i\epsilon} \left(\frac{1}{n_4} - \frac{1}{n_2} \right) \left(\frac{1}{n_5} + \frac{1}{n_6} - \frac{1}{n_3} \right) + \frac{1}{\omega_{p_2, p_6; p_4} + i\epsilon} \left(\frac{1}{n_5} - \frac{1}{n_3} \right) \left(\frac{1}{n_4} - \frac{1}{n_2} - \frac{1}{n_6} \right) \right] \right. \\
& - \frac{1}{n_2} \frac{1}{\omega_{p_3, p_4; p_1, p_6} + i\epsilon} \left[\frac{1}{\omega_{p_3; p_5, p_6} + i\epsilon} \left(\frac{1}{n_1} - \frac{1}{n_4} \right) \left(\frac{1}{n_5} + \frac{1}{n_6} - \frac{1}{n_3} \right) + \frac{1}{\omega_{p_4, p_5; p_1} + i\epsilon} \left(\frac{1}{n_6} - \frac{1}{n_3} \right) \left(\frac{1}{n_1} - \frac{1}{n_4} - \frac{1}{n_5} \right) \right] \\
& \left. - \frac{1}{n_3} \frac{1}{\omega_{p_2, p_5, p_6; p_1} + i\epsilon} \left[\frac{1}{\omega_{p_4, p_5; p_1} + i\epsilon} \left(\frac{-1}{n_2} - \frac{1}{n_6} \right) \left(\frac{1}{n_1} - \frac{1}{n_4} - \frac{1}{n_5} \right) + \frac{1}{\omega_{p_2, p_6; p_4} + i\epsilon} \left(\frac{1}{n_1} - \frac{1}{n_5} \right) \left(\frac{-1}{n_2} + \frac{1}{n_4} - \frac{1}{n_6} \right) \right] \right\}, \tag{3.9}
\end{aligned}$$

where the six terms arise from the $3!$ possible orderings of the times $t_b, t_c, t_d > t_a$. In particular, the time orderings of the six terms are: $t_b > t_d > t_c$, $t_d > t_b > t_c$, $t_b > t_c > t_d$, $t_c > t_b > t_d$, $t_c > t_d > t_b$, $t_d > t_c > t_b$, from first to last, respectively. In fact, as a result of the symmetries of the tetrahedron, each of the six terms can be obtained by a symmetry transformation of one another, see Appendix B.

In addition to this diagram, there is the same tetrahedron diagram but with the arrow on line 5 reversed. The result for the latter can be obtained from the former in a simple way, from symmetry, and is also discussed in Appendix B.

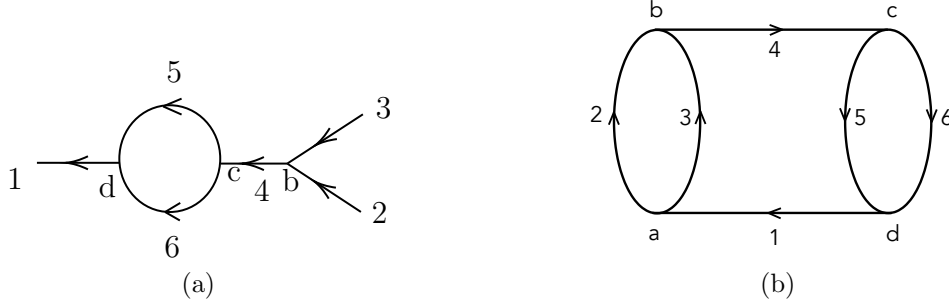


Figure 4: (a) A one-loop diagram contributing to the three-point function. (b) We set the external times to be equal to t_a , represented by the three lines meeting at the point t_a .

Propagator renormalization

Now we look at the loop diagram shown in Fig. 4 which can be viewed as arising from propagator renormalization. We find that its contribution to the equal-time three-point function is,

$$\begin{aligned}
& \frac{-1}{2} \sum_{p_4, p_5, p_6} \lambda_{423} \lambda_{456}^* \lambda_{156} \prod_{i=1}^6 n_i \frac{1}{\omega_{p_2, p_3; p_1} + i\epsilon} \left\{ \frac{1}{\omega_{p_2, p_3; p_4} + i\epsilon} \frac{1}{\omega_{p_2, p_3; p_5, p_6} + i\epsilon} \frac{1}{n_1} \left(\frac{1}{n_5} + \frac{1}{n_6} \right) \left(\frac{1}{n_2} + \frac{1}{n_3} - \frac{1}{n_4} \right) \right. \\
& - \frac{1}{\omega_{p_4; p_5, p_6} + i\epsilon} \left(\frac{1}{\omega_{p_2, p_3; p_5, p_6} + i\epsilon} + \frac{1}{\omega_{p_4; p_1} + i\epsilon} \right) \frac{1}{n_1} \left(\frac{1}{n_2} + \frac{1}{n_3} \right) \left(\frac{1}{n_4} - \frac{1}{n_5} - \frac{1}{n_6} \right) \\
& \left. + \frac{1}{\omega_{p_5, p_6; p_1} + i\epsilon} \frac{1}{\omega_{p_4; p_1} + i\epsilon} \frac{1}{n_4} \left(\frac{1}{n_2} + \frac{1}{n_3} \right) \left(\frac{1}{n_5} + \frac{1}{n_6} - \frac{1}{n_1} \right) \right\}, \quad (3.10)
\end{aligned}$$

where the terms correspond to the time orderings $t_b > t_c > t_d$, $t_c > t_b > t_d$, $t_c > t_d > t_b$, $t_d > t_c > t_b$ from first to last, respectively.⁷

There are several more diagrams of this kind, which can be viewed as a symmetry transformation of this diagram, as we will see below. In fact, in (3.10) one should, by momentum conservation, set $p_4 = p_1$. This gives some terms that are divergent. Specifically, (3.10) gives the term,

$$\frac{-1}{i\epsilon} \frac{1}{2} \sum_{1, \dots, 6} \lambda_{123} |\lambda_{156}|^2 \prod_{i=1}^6 n_i \frac{1}{\omega_{p_2, p_3; p_1} + i\epsilon} \frac{1}{n_1} \left(\frac{1}{n_2} + \frac{1}{n_3} \right) 2\pi i \delta(\omega_{p_1; p_5, p_6}) \left(\frac{1}{n_1} - \frac{1}{n_5} - \frac{1}{n_6} \right). \quad (3.11)$$

However, these terms cancel when including the diagram Fig. 5(b) that will be shown in the next section, provided that one uses that the state is stationary, as governed by the leading order kinetic equation. In particular, adding to (3.11) the corresponding divergent contribution of the diagram

⁷The combinatorial factor of 1/2 out front is: 1/8 because each vertex comes with a 1/2, then a combinatorial factor of 2 from the loop integral, and a factor of 2 from exchanging 2 and 3 when contracting with the external legs.

Fig. 5(b) gives,

$$\frac{-1}{i\epsilon} \frac{1}{2} \sum_{1,\dots,6} \lambda_{123} \prod_{i=1}^6 n_i \frac{1}{\omega_{p_2,p_3;p_1} + i\epsilon} \frac{1}{n_1} \left(\frac{1}{n_2} + \frac{1}{n_3} \right) \left[|\lambda_{156}|^2 2\pi i \delta(\omega_{p_1;p_5,p_6}) \left(\frac{1}{n_1} - \frac{1}{n_5} - \frac{1}{n_6} \right) + 2|\lambda_{615}|^2 2\pi i \delta(\omega_{p_1 p_5; p_6}) \left(\frac{1}{n_1} + \frac{1}{n_5} - \frac{1}{n_6} \right) \right]. \quad (3.12)$$

However, the term in brackets vanishes by the tree-level kinetic equation. This is a useful illustration of the fact that all our computations are of equal-time correlation functions, assuming a stationary state.

3.3. Next-to-leading order kinetic equation for cubic interactions

We are now ready to write down the kinetic equation to next-to-leading order. It follows from the equal-time three-point function, via (2.20). The complex conjugate version of this equation is,

$$\frac{\partial n_k}{\partial t} = - \sum_{p_1, p_2, p_3} (\delta_{kp_1} - \delta_{kp_2} - \delta_{kp_3}) \text{Im} \left(\lambda_{123}^* \langle a_{p_1} a_{p_2}^\dagger a_{p_3}^\dagger \rangle \right). \quad (3.13)$$

The three-point function consists of an infinite sequence of terms, grouped by their order in λ , and we go up to order λ^3 ,

$$\langle a_{p_1} a_{p_2}^\dagger a_{p_3}^\dagger \rangle = \langle a_{p_1} a_{p_2}^\dagger a_{p_3}^\dagger \rangle_\lambda + \langle a_{p_1} a_{p_2}^\dagger a_{p_3}^\dagger \rangle_{\lambda^3} \quad (3.14)$$

$$\langle a_{p_1} a_{p_2}^\dagger a_{p_3}^\dagger \rangle_\lambda = \lambda_{123} \frac{1}{\omega_{p_2,p_3;p_1} + i\epsilon} n_1 n_2 n_3 \left(\frac{1}{n_1} - \frac{1}{n_2} - \frac{1}{n_3} \right) \quad (3.15)$$

$$\langle a_{p_1} a_{p_2}^\dagger a_{p_3}^\dagger \rangle_{\lambda^3} = V_a + V_b + P_a + P_b + P_c + P_d + P_e \quad (3.16)$$

The leading order term $\langle a_{p_1} a_{p_2}^\dagger a_{p_3}^\dagger \rangle_\lambda$, given earlier in (2.18), gives the standard (leading order) kinetic equation. The next-to-leading order term $\langle a_{p_1} a_{p_2}^\dagger a_{p_3}^\dagger \rangle_{\lambda^3}$ gives the first corrections to this. The terms appearing here are: V_a , which arises from the diagram shown earlier in Fig. 3(a), V_b which comes from Fig. 3(a) but with the arrow on line 5 reversed, P_a which comes from the diagram shown earlier in Fig. 4(a) and shown again in Fig. 5(a), and P_b, P_c, P_d, P_e which have different choices of arrows on the propagator renormalization loop and different choices of lines

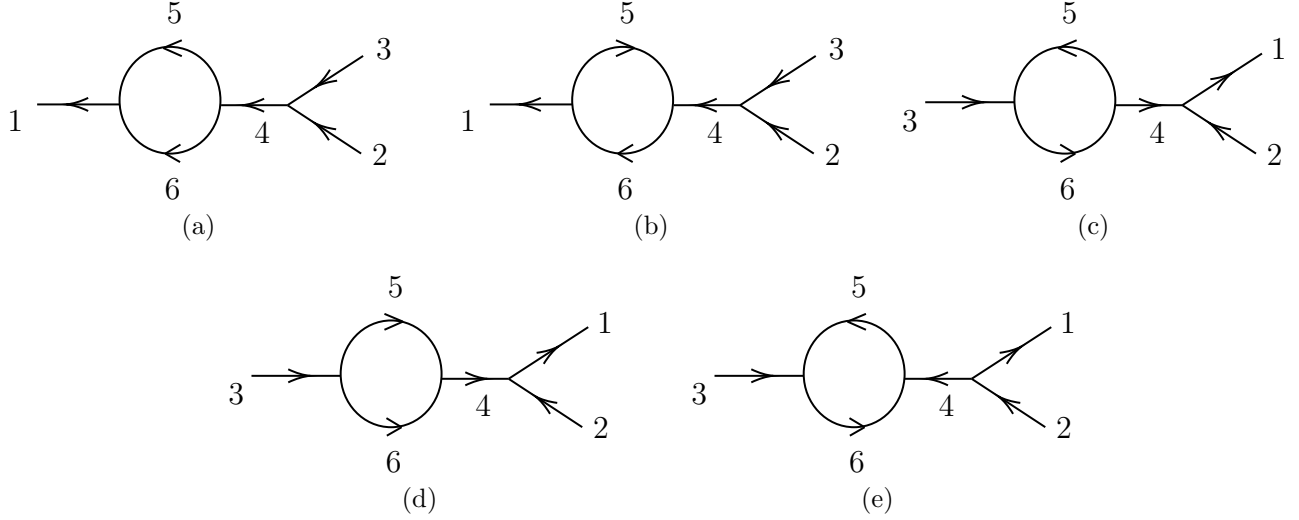


Figure 5: The different propagator renormalization diagrams contributing to the three-point functions. All the diagrams can be obtained from a (whose contribution is denoted by P_a) through symmetry transformations, see Appendix B. In particular, we get P_b from P_a by sending $5 \rightarrow -5$. We get P_c and P_d from P_a and P_b , respectively, by sending $1 \leftrightarrow -3$ and $6 \rightarrow -6$ (and also $4 \rightarrow -4$, however 4 in a is just 1). Finally, we get diagram e from diagram a by sending $1 \leftrightarrow -3$ and $6 \rightarrow -6$. Note that diagrams c, d, e have a propagator renormalization for line 3. We could have alternatively put it on line 2; we account for this by adding a factor of 2 for P_c, P_d, P_e .

which get the propagator renormalization. Explicitly,

$$\begin{aligned}
V_a = & 2 \sum_{p_4, p_5, p_6} \lambda_{426} \lambda_{356}^* \lambda_{145} \prod_{i=1}^6 n_i \frac{1}{\omega_{p_2, p_3; p_1} + i\epsilon} \\
& \left\{ \frac{1}{n_1} \frac{1}{\omega_{p_2, p_3; p_4, p_5} + i\epsilon} \left[\frac{1}{\omega_{p_3; p_5; p_6} + i\epsilon} \left(\frac{1}{n_4} - \frac{1}{n_2} \right) \left(\frac{1}{n_5} + \frac{1}{n_6} - \frac{1}{n_3} \right) + \frac{1}{\omega_{p_2, p_6; p_4} + i\epsilon} \left(\frac{1}{n_5} - \frac{1}{n_3} \right) \left(\frac{1}{n_4} - \frac{1}{n_2} - \frac{1}{n_6} \right) \right] \right. \\
& - \frac{1}{n_2} \frac{1}{\omega_{p_3; p_4; p_1, p_6} + i\epsilon} \left[\frac{1}{\omega_{p_3; p_5; p_6} + i\epsilon} \left(\frac{1}{n_1} - \frac{1}{n_4} \right) \left(\frac{1}{n_5} + \frac{1}{n_6} - \frac{1}{n_3} \right) + \frac{1}{\omega_{p_4, p_5; p_1} + i\epsilon} \left(\frac{1}{n_6} - \frac{1}{n_3} \right) \left(\frac{1}{n_1} - \frac{1}{n_4} - \frac{1}{n_5} \right) \right] \\
& \left. - \frac{1}{n_3} \frac{1}{\omega_{p_2, p_5; p_6; p_1} + i\epsilon} \left[\frac{1}{\omega_{p_4, p_5; p_1} + i\epsilon} \left(\frac{-1}{n_2} - \frac{1}{n_6} \right) \left(\frac{1}{n_1} - \frac{1}{n_4} - \frac{1}{n_5} \right) + \frac{1}{\omega_{p_2, p_6; p_4} + i\epsilon} \left(\frac{1}{n_1} - \frac{1}{n_5} \right) \left(\frac{-1}{n_2} + \frac{1}{n_4} - \frac{1}{n_6} \right) \right] \right\}
\end{aligned}$$

$$\begin{aligned}
V_b = & 2 \sum_{p_4, p_5, p_6} \lambda_{426} \lambda_{635} \lambda_{451}^* \prod_{i=1}^6 n_i \frac{1}{\omega_{p_2, p_3; p_1} + i\epsilon} \\
& \left\{ \frac{1}{n_1} \frac{1}{\omega_{p_2, p_3; p_5; p_4} + i\epsilon} \left[\frac{1}{\omega_{p_3; p_5; p_6} + i\epsilon} \left(\frac{1}{n_4} - \frac{1}{n_2} \right) \left(\frac{-1}{n_5} + \frac{1}{n_6} - \frac{1}{n_3} \right) + \frac{1}{\omega_{p_2, p_6; p_4} + i\epsilon} \left(\frac{-1}{n_5} - \frac{1}{n_3} \right) \left(\frac{1}{n_4} - \frac{1}{n_2} - \frac{1}{n_6} \right) \right] \right. \\
& - \frac{1}{n_2} \frac{1}{\omega_{p_3; p_4; p_1, p_6} + i\epsilon} \left[\frac{1}{\omega_{p_3; p_5; p_6} + i\epsilon} \left(\frac{1}{n_1} - \frac{1}{n_4} \right) \left(\frac{-1}{n_5} + \frac{1}{n_6} - \frac{1}{n_3} \right) + \frac{1}{\omega_{p_4; p_1, p_5} + i\epsilon} \left(\frac{1}{n_6} - \frac{1}{n_3} \right) \left(\frac{1}{n_1} - \frac{1}{n_4} + \frac{1}{n_5} \right) \right] \\
& \left. - \frac{1}{n_3} \frac{1}{\omega_{p_2, p_6; p_1, p_5} + i\epsilon} \left[\frac{1}{\omega_{p_4; p_1, p_5} + i\epsilon} \left(\frac{-1}{n_2} - \frac{1}{n_6} \right) \left(\frac{1}{n_1} - \frac{1}{n_4} + \frac{1}{n_5} \right) + \frac{1}{\omega_{p_2, p_6; p_4} + i\epsilon} \left(\frac{1}{n_1} + \frac{1}{n_5} \right) \left(\frac{-1}{n_2} + \frac{1}{n_4} - \frac{1}{n_6} \right) \right] \right\}
\end{aligned}$$

$$P_a = -\frac{1}{2} \sum_{p_5, p_6} \lambda_{123} |\lambda_{156}|^2 \prod_{i=1}^3 n_i n_5 n_6 \frac{1}{\omega_{p_2, p_3; p_1} + i\epsilon} \frac{1}{\omega_{p_2, p_3; p_5, p_6} + i\epsilon} \left[\frac{1}{\omega_{p_2, p_3; p_1} + i\epsilon} \left(\frac{1}{n_5} + \frac{1}{n_6} \right) \left(\frac{1}{n_2} + \frac{1}{n_3} - \frac{1}{n_1} \right) - \frac{1}{\omega_{p_1; p_5, p_6} + i\epsilon} \left(\frac{1}{n_2} + \frac{1}{n_3} \right) \left(\frac{1}{n_1} - \frac{1}{n_5} - \frac{1}{n_6} \right) \right]$$

$$P_b = -\sum_{p_5, p_6} \lambda_{123} |\lambda_{651}|^2 \prod_{i=1}^3 n_i n_5 n_6 \frac{1}{\omega_{p_2, p_3; p_1} + i\epsilon} \frac{1}{\omega_{p_2, p_3; p_5, p_6} + i\epsilon} \left[\frac{1}{\omega_{p_2, p_3; p_1} + i\epsilon} \left(\frac{-1}{n_5} + \frac{1}{n_6} \right) \left(\frac{1}{n_2} + \frac{1}{n_3} - \frac{1}{n_1} \right) - \frac{1}{\omega_{p_1; p_5, p_6} + i\epsilon} \left(\frac{1}{n_2} + \frac{1}{n_3} \right) \left(\frac{1}{n_1} + \frac{1}{n_5} - \frac{1}{n_6} \right) \right]$$

$$P_c = 2 \sum_{p_5, p_6} \lambda_{123} |\lambda_{653}|^2 \prod_{i=1}^3 n_i n_5 n_6 \frac{1}{\omega_{p_2, p_3; p_1} + i\epsilon} \frac{1}{\omega_{p_2, p_6; p_1, p_5} + i\epsilon} \left[\frac{1}{\omega_{p_2, p_3; p_1} + i\epsilon} \left(\frac{1}{n_5} - \frac{1}{n_6} \right) \left(\frac{1}{n_2} + \frac{1}{n_3} - \frac{1}{n_1} \right) - \frac{1}{\omega_{p_6; p_3, p_5} + i\epsilon} \left(\frac{1}{n_2} - \frac{1}{n_1} \right) \left(\frac{-1}{n_3} - \frac{1}{n_5} + \frac{1}{n_6} \right) \right]$$

$$P_d = \sum_{p_5, p_6} \lambda_{123} |\lambda_{356}|^2 \prod_{i=1}^3 n_i n_5 n_6 \frac{1}{\omega_{p_2, p_3; p_1} + i\epsilon} \frac{1}{\omega_{p_2, p_5; p_6; p_1} + i\epsilon} \left[\frac{1}{\omega_{p_2, p_3; p_1} + i\epsilon} \left(\frac{-1}{n_5} - \frac{1}{n_6} \right) \left(\frac{1}{n_2} + \frac{1}{n_3} - \frac{1}{n_1} \right) - \frac{1}{\omega_{p_5; p_6; p_3} + i\epsilon} \left(\frac{1}{n_2} - \frac{1}{n_1} \right) \left(\frac{-1}{n_3} + \frac{1}{n_5} + \frac{1}{n_6} \right) \right]$$

$$P_e = -2 \sum_{p_5, p_6} \lambda_{213}^* \lambda_{536} \lambda_{635} \prod_{i=1}^3 n_i n_5 n_6 \frac{1}{\omega_{p_2, p_3; p_1} + i\epsilon} \left\{ -\frac{1}{\omega_{p_2; p_1, p_3} + i\epsilon} \frac{1}{\omega_{p_2, p_6; p_1, p_5} + i\epsilon} \left(\frac{1}{n_5} - \frac{1}{n_6} \right) \left(\frac{1}{n_2} - \frac{1}{n_1} - \frac{1}{n_3} \right) + \frac{1}{\omega_{p_3, p_6; p_5} + i\epsilon} \left(\frac{1}{\omega_{p_2, p_6; p_1, p_5} + i\epsilon} + \frac{1}{2\omega_{p_3} + i\epsilon} \right) \left(\frac{1}{n_2} - \frac{1}{n_1} \right) \left(\frac{1}{n_3} - \frac{1}{n_5} + \frac{1}{n_6} \right) + \frac{1}{\omega_{p_3, p_5; p_6} + i\epsilon} \frac{1}{2\omega_{p_3} + i\epsilon} \left(\frac{1}{n_2} - \frac{1}{n_1} \right) \left(\frac{1}{n_5} - \frac{1}{n_6} + \frac{1}{n_3} \right) \right\}.$$

Further discussion of terms in the kinetic equation is given in Appendix C.

4. Prescription for a general Feynman diagram

In this section we give an algorithm for computing the contribution of any Feynman diagram to an equal-time correlation function. In Sec. 2 we already showed that correlation functions can be computed order by order in the nonlinear interaction (λ), just as one does in quantum field theory. The remaining task is, for a given Feynman diagram, to perform the integration over the

intermediate times (or, equivalently, frequencies) appearing in the loops. We did this explicitly in the previous section, for some particular one loop diagrams. From the several diagrams that we evaluated, we can deduce the rule for a general diagram. We first state the rules and then derive them.

Rules:

1. Pick an ordering of the times at each vertex. The time t_a at which the correlation function is being evaluated must be the smallest time.
2. Start at the latest time on the diagram and move from vertex to vertex in decreasing order of their times, until finally reaching the vertex at the earliest time. Each next vertex must be a neighbor of at least one previously visited vertex.
3. At each step in this process, draw an imaginary loop enclosing all vertices visited so far. Write down a factor of

$$\frac{-1}{\omega_{p_i} + \omega_{p_j} + \dots - \omega_{p_a} - \omega_{p_b} - \dots + i\epsilon}, \quad (4.1)$$

where $\omega_i, \omega_j, \dots$ are the frequencies of all lines entering this imaginary loop and $\omega_a, \omega_b, \dots$ are the frequencies of all lines leaving the imaginary loop.

4. In addition, at each step in the process, write down a factor of

$$\left(\frac{1}{n_k} + \frac{1}{n_l} + \dots - \frac{1}{n_\alpha} - \frac{1}{n_\beta} - \dots \right), \quad (4.2)$$

where $\omega_k, \omega_l, \dots$ are the frequencies of the lines entering the vertex and $\omega_\alpha, \omega_\beta$ are the frequencies of the lines leaving the vertex. However, omit an $\frac{1}{n_i}$ if it has already been included at a previous step.

5. Multiply the resulting expression by a product of n_i , one for each frequency ω_i appearing in the diagram, and multiply by a product of the couplings for each vertex, and sum the resulting expression over all internal momenta.
6. Repeat Step 1 through 5 for all possible time orderings and sum the results. Include the appropriate Feynman diagram combinatorics factor.

Justification: Let us understand these rules. Suppose for concreteness that we have four vertices with the time ordering $t_d > t_c > t_b > t_a$. The integrals we need to do are,

$$\int_{t_a}^{\infty} dt_b e^{-i\sigma_b t_b} \int_{t_b}^{\infty} dt_c e^{-i\sigma_c t_c} \int_{t_c}^{\infty} dt_d e^{-i\sigma_d t_d} = \frac{-i}{(\sigma_b + \sigma_c + \sigma_d)} \frac{-i}{(\sigma_c + \sigma_d)} \frac{-i}{\sigma_d}. \quad (4.3)$$

Here the σ are the sum of the outgoing minus ingoing frequencies from a vertex; we get these through the delta functions we insert, see below (3.1). One now sees that as we successively do the integrals, starting from the latest time, we get the rules listed in Steps 2 and 3. Note that all our integrals here converge (because the relevant poles of the ω integrals were chosen to ensure this), so the contributions from infinite time vanish.

Now let us understand the vertex factor, appearing in Step 4. According to the Feynman rules, each vertex comes with a sum of g_i^* for each propagator leaving the vertex and a $-g_i$ for each propagator entering the vertex, see (2.14). At the poles, $\omega_i = \omega_{p_i} \pm \gamma_i$, we see from (2.13) that g_i and g_i^* become,

$$g_i \rightarrow \begin{cases} \frac{1}{n_i}, & \omega_i = \omega_{p_i} + i\gamma_i \\ 0, & \omega_i = \omega_{p_i} - i\gamma_i \end{cases} \quad g_i^* \rightarrow \begin{cases} 0, & \omega_i = \omega_{p_i} + i\gamma_i \\ \frac{1}{n_i}, & \omega_i = \omega_{p_i} - i\gamma_i \end{cases}. \quad (4.4)$$

So from each vertex we will get a sum and difference of various $1/n_i$. We need only determine if for a propagator entering or leaving a vertex we get a $1/n_i$ or nothing. Consider two vertices next to each other, as in Fig. 2(a). In the corresponding vertex factor (3.1), either the $g_5 + g_6$ term coming from vertex b gives $1/n_5 + 1/n_6$ and the $g_5^* + g_6^*$ term coming from vertex c gives 0, or vice-versa. Which option is the correct one depends on the time ordering of t_b and t_c , which determines if the ω_5, ω_6 integrals are closed in the upper or lower half plane. In particular, the vertex at the later time gets to have the $1/n_5 + 1/n_6$. Since in our prescription we proceed from later to earlier time, this explains Step 4.

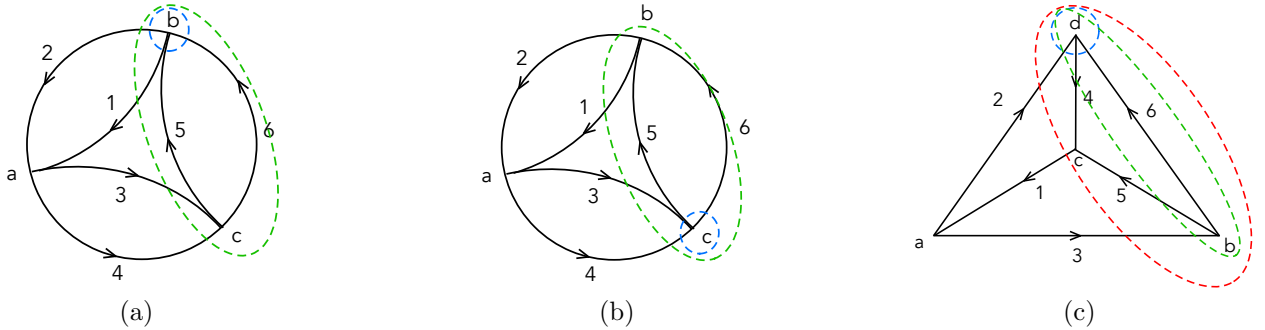


Figure 6: Applying the rules to four-point and three-point correlation functions.

Examples: Let us look at some examples of applying these rules. Consider again the one-loop diagram for the quartic interaction, Fig. 2. Take the time ordering $t_b > t_c > t_a$. We draw a loop around vertex b , shown in blue in Fig. 6(a). Step 3 instructs us to write a factor of

$$\frac{-1}{\omega_{p_5, p_6; p_1, p_2} + i\epsilon}, \quad (4.5)$$

and Step 4 instructs us to write a factor of

$$\left(\frac{1}{n_5} + \frac{1}{n_6} - \frac{1}{n_1} - \frac{1}{n_2} \right). \quad (4.6)$$

The next largest time is t_c , so we expand our loop (shown in green) to include vertex c . Step 3 instructs us to write a factor of

$$\frac{-1}{\omega_{p_3, p_4; p_1, p_2} + i\epsilon}, \quad (4.7)$$

and Step 4 instructs us to write a factor of

$$\left(\frac{1}{n_3} + \frac{1}{n_4} \right). \quad (4.8)$$

As Step 4 says, even though ω_1 and ω_2 are leaving the green circle, we do not include $-\frac{1}{n_1} - \frac{1}{n_2}$ since this term already appeared earlier, when accounting for the blue loop around vertex b , (4.6). Implementing Step 5, we reproduce (3.5). The other time ordering, $t_c > t_b > t_a$, proceeds in a similar fashion. We have drawn the corresponding loops in Fig. 6(b).

Let us now look again at the loop digram for the cubic interaction, Fig. 3, which we evaluated earlier. There are six possible time orderings. Let us look at, for instance, the one in which $t_d > t_b > t_c > t_a$. We draw a loop, shown in green in Fig. 6(c), around vertex d , which is at the latest time. Frequencies ω_2 and ω_6 are entering and ω_4 is leaving. Steps 3 and 4 instruct us to write a factor of

$$\frac{-1}{\omega_{p_2, p_6; p_4} + i\epsilon} \left(\frac{1}{n_2} + \frac{1}{n_6} - \frac{1}{n_4} \right). \quad (4.9)$$

Expanding the loop to include the vertex b , which is at the next largest time, we get the loop shown in green in Fig. 6(c). Frequencies ω_2 and ω_3 are entering and ω_4 and ω_5 are leaving. Steps 3 and 4 instruct us to write a factor of

$$\frac{-1}{\omega_{p_2, p_3; p_4, p_5} + i\epsilon} \left(\frac{1}{n_3} - \frac{1}{n_5} \right), \quad (4.10)$$

where there is no $1/n_2 - 1/n_4$, since it was already included in (4.9). Finally, we expand the loop to the loop shown in red in Fig. 6(c), so as to include vertex c . Frequencies ω_2 and ω_3 are entering and ω_1 is leaving. Steps 3 and 4 instruct us to write a factor of

$$\frac{-1}{\omega_{p_2, p_3; p_1} + i\epsilon} \frac{1}{n_1}, \quad (4.11)$$

where there is no $1/n_2$ or $1/n_3$, since both were already included. Multiplying (4.9), (4.10), and (4.11), we reproduce the second of the six terms in (3.9).

As our final example, let us look at an example of a diagram that occurs if we have both cubic

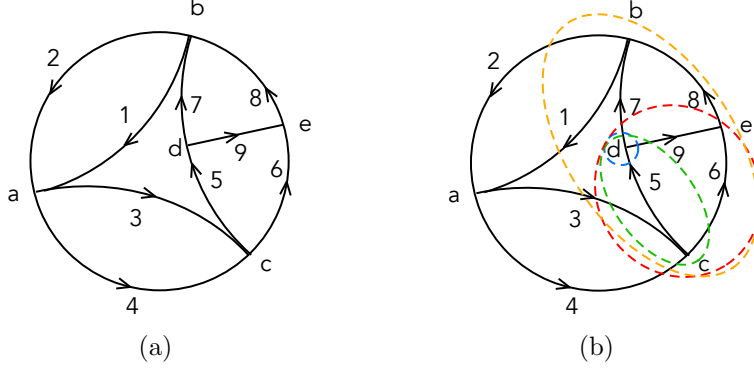


Figure 7: (a) An example of a higher order diagram. (b) Applying our rules to a particular time ordering, resulting in the contribution (4.12).

and quartic interactions. One such diagram (chosen for no particular reason) is shown in Fig. 7 (a). It contributes to the equal time four-point function $\langle a_1 a_2 a_3^\dagger a_4^\dagger \rangle(t_a)$. There are many different time orderings one needs to consider. To illustrate, let us pick one such ordering: $t_d > t_c > t_e > t_b > t_a$. Applying the rules we get the contribution,

$$\sum_{p_i} \lambda_{1278} \lambda_{5634} \lambda_{869} \lambda_{579}^* \prod_{i=1}^9 n_i \frac{-1}{\omega_{p_5; p_7, p_9} + i\epsilon} \left(\frac{1}{n_5} - \frac{1}{n_7} - \frac{1}{n_9} \right) \frac{-1}{\omega_{p_3, p_4; p_6, p_7, p_9} + i\epsilon} \left(\frac{1}{n_3} + \frac{1}{n_4} - \frac{1}{n_6} \right) \frac{-1}{\omega_{p_3, p_4; p_7, p_8} + i\epsilon} \left(-\frac{1}{n_8} \right) \frac{-1}{\omega_{p_3, p_4; p_1, p_2} + i\epsilon} \left(-\frac{1}{n_1} - \frac{1}{n_2} \right), \quad (4.12)$$

where reading from left to right, the terms correspond to larger and larger loops shown in Fig. 7 (b).

5. Discussion

In [18] we gave a systematic method for computing higher order terms in the wave kinetic equation: correlation functions are defined by averaging over Gaussian random forcing, which is set to zero at the end. This stochastic classical field theory is equivalent to a quantum field theory. One computes equal-time correlation functions in the quantum field theory, order by order in the number of interaction vertices, and inserts into the right hand side of (2.20) to get the kinetic equation. The only nontrivial step is evaluating the Feynman diagrams with loops, which involve integrals over the intermediate times (or frequencies) inside the loops. In this paper we have shown how to carry out the integrals in general, obtaining a simple prescription for writing the result, described in Sec. 4.

Our answer still has integrals over the loop momenta; these need to be done on a case by case basis, as they are functions of the couplings, $\lambda_{p_1 p_2 p_3}$ and $\lambda_{p_1 p_2 p_3 p_4}$, which are momentum dependent and system dependent. If these loop integrals over momenta didn't have UV or IR divergences, we

would be close to being done — the corrections to the leading order kinetic equation would always be small, and the largest corrections would come from the loop diagrams with the fewest number of interaction vertices. But we’re not done: the loops often have UV and IR divergences [19]. This introduces additional small and large parameters which compete with the smallness of the nonlinearity parameter, and make the perturbation theory multiscale. We must decide which classes of loop diagrams are dominant and sum those. In other words, we must renormalize. The results in this paper provide the necessary tools to carry out this task, which will be the subject of future work.

Acknowledgments

We thank G. Falkovich for many discussions and collaboration on related work. This work is supported in part by NSF grant PHY-2209116, by BSF grant 2022113, and by the ITS through a Simons grant. The work of MS is supported by the Israeli Science Foundation Center of Excellence (grant No. 2289/18). VR and MS thank the Aspen Center for Physics (NSF grant PHY-2210452) where part of this work was completed.

A. Perturbative Liouville equation for waves

An alternate method for studying wave turbulence is to average over phase space, instead of introducing external forcing and dissipation. In particular, one aims to find the evolution of the phase space density $\rho(J_i, \alpha_i, t)$, a function of the action, J_i , and angle, α_i , variables, with i running over the different modes of the field. This method was used in [20] to find the next-to-leading order correction to the kinetic equation for a theory with four-wave interactions. Here we extend this to the theory with three-wave interactions, like the one studied in the main body, reproducing the results found there. In fact, we go further: we show that at every order in perturbation theory, the results of this method agree with the one in the main body of the text.⁸

Perturbative solution of the Liouville equation

The evolution of the phase space density is governed by the Liouville equation [11],

$$i \frac{\partial \rho}{\partial t} = (L_0 + \delta L) \rho, \tag{A.1}$$

$$L_0 = -i\vec{\omega} \cdot \frac{\partial}{\partial \vec{\alpha}}, \quad \delta L = i \left(\frac{\partial H_{int}}{\partial \vec{\alpha}} \cdot \frac{\partial}{\partial \vec{J}} - \frac{\partial H_{int}}{\partial \vec{J}} \cdot \frac{\partial}{\partial \vec{\alpha}} \right), \tag{A.2}$$

⁸An alternate way of seeing the equivalence, which will be discussed in [27], is to solve for the complete evolution of the phase space density when one has random forcing (the Fokker-Planck equation), and then either first average over forcing and then phase space, or vice-versa.

where L_0 is due to the free part of the Hamiltonian, H_2 (which only depends on the action variables), and δL is due to the interacting part, H_{int} . We have defined, $\omega_j \equiv \frac{\partial H_2}{\partial J_j}$.

The solution for a time-independent phase space density is given by iterating,

$$\langle \vec{n} | \Phi \rangle = \langle \vec{n} | \Phi_0 \rangle + \sum_{\vec{n}'} G(\vec{n}) \langle \vec{n} | \delta L | \vec{n}' \rangle \langle \vec{n}' | \Phi \rangle, \quad (\text{A.3})$$

where the eigenfunctions $|\vec{n}\rangle$ of the free Liouville operator L_0 are plane waves $\langle \vec{\alpha} | \vec{n} \rangle = \exp(i\vec{n} \cdot \vec{\alpha})$ and $G(\vec{n})$ is the propagator,

$$G(\vec{n}) = \frac{1}{-\vec{n} \cdot \vec{\omega} + i\epsilon}. \quad (\text{A.4})$$

The kinetic equation is then given by,

$$\frac{\partial n_r}{\partial t} \propto \int dJ J_r \delta \mathcal{L}, \quad \text{where } \delta \mathcal{L} = \sum_{\vec{n}'} \langle \vec{0} | \delta L | \vec{n}' \rangle \langle \vec{n}' | \Phi \rangle. \quad (\text{A.5})$$

Inserting (A.3) gives $\delta \mathcal{L} = (\delta \mathcal{L})_{\text{first}} + (\delta \mathcal{L})_{\text{second}} + \dots$, where

$$(\delta \mathcal{L})_{\text{first}} = \sum_{\vec{n}'} \langle \vec{0} | \delta L | \vec{n}' \rangle G(\vec{n}') \langle \vec{n}' | \delta L | 0 \rangle \rho(J) \quad (\text{A.6})$$

$$(\delta \mathcal{L})_{\text{second}} = \sum_{\vec{n}', \vec{n}''} \langle \vec{0} | \delta L | \vec{n}' \rangle G(\vec{n}') \langle \vec{n}' | \delta L | \vec{n}'' \rangle G(\vec{n}'') \langle \vec{n}'' | \delta L | 0 \rangle \rho(J) + \dots \quad (\text{A.7})$$

where $\rho(J) \equiv \langle 0 | \Phi_0 \rangle$. We will take $\rho(J)$ to be a Gaussian,

$$\rho(J) = \frac{1}{\prod_i n_i} \exp\left(-\sum_i \frac{J_i}{n_i}\right), \quad \langle J_i \rangle = n_i, \quad (\text{A.8})$$

The main point is this: the phase space integrated over all angles, $\rho(J)$, which has no angular dependence, is governed by a differential equation, the right-hand side of which encodes a series of transitions to intermediate states which have angular dependence. In particular, each interaction vertex gives q of the different modes angular dependence (for a q -body interaction). We start and end in a state with no angular dependence.

In [20] we specialized these equations to interacting waves with a quartic interaction. Here we look at these equations for a field theory with a cubic interaction. The Hamiltonian, $H_2 + H_3$, takes the following form when written in action-angle variables, $a_p = \sqrt{J_p} e^{-i\alpha_p}$,

$$H = \sum_p \omega_p J_p + \frac{1}{2} \sum_{p_i} \sqrt{J_1 J_2 J_3} \left(\lambda_{123} e^{i(\alpha_1 - \alpha_2 - \alpha_3)} + \text{c.c.} \right). \quad (\text{A.9})$$

Computing the Liouville operator we have that L_0 is (A.2) with ω_i given by ω_p and δL in (A.2) is

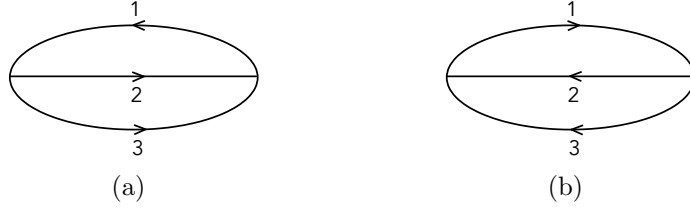


Figure 8: Intermediate states (a) $|\bar{1}; 23\rangle$, and (b) $|\bar{2}\bar{3}; 1\rangle$. Our notation is such that when we write $|\bar{1}; 23\rangle$ we mean a state in which mode 1 has occupation number -1 and modes 2 and 3 have occupation number 1.

equal to,

$$\delta L = \frac{1}{2} \sum_{1,2,3} (-\lambda_{123}) \sqrt{J_1 J_2 J_3} e^{-i\vec{e}_{1,2,3} \cdot \vec{\alpha}} \left[(\partial_1 - \partial_2 - \partial_3) + \frac{i}{2} \left(\frac{\partial_{\alpha_1}}{J_1} + \frac{\partial_{\alpha_2}}{J_2} + \frac{\partial_{\alpha_3}}{J_3} \right) \right] - \text{c.c.} , \quad (\text{A.10})$$

where $\partial_i \equiv \partial_{J_i}$ and where $\vec{e}_{i,j,k}$, which is a vector that has a -1 in the i 'th entry and a $+1$ in the j 'th and k 'th, and a zero elsewhere; in other words, $-\vec{e}_{i,j,k} \cdot \vec{\alpha} = \alpha_i - \alpha_j - \alpha_k$. The matrix element of δL trivially follows,

$$\begin{aligned} \langle \vec{n} | \delta L | \vec{n}' \rangle &= -\frac{1}{2} \sum_{1,2,3} \lambda_{123} \sqrt{J_1 J_2 J_3} \delta_{\vec{n} + \vec{e}_{1,2,3}, \vec{n}'} \left[(\partial_1 - \partial_2 - \partial_3) - \frac{1}{2} \left(\frac{n'_1}{J_1} + \frac{n'_2}{J_2} + \frac{n'_3}{J_3} \right) \right] \\ &\quad - \frac{1}{2} \sum_{1,2,3} \lambda_{123}^* \sqrt{J_1 J_2 J_3} \delta_{\vec{n} + \vec{e}_{2,3,1}, \vec{n}'} \left[(\partial_2 + \partial_3 - \partial_1) - \frac{1}{2} \left(\frac{n'_1}{J_1} + \frac{n'_2}{J_2} + \frac{n'_3}{J_3} \right) \right] , \quad (\text{A.11}) \end{aligned}$$

where $\vec{e}_{2,3,1} = -\vec{e}_{1,2,3}$.

Leading order

We now start iteratively computing the kinetic equation (A.5), starting with $(\delta \mathcal{L})_{\text{first}}$ in (A.6). There are two diagrams, as shown in Fig. 8. The first, Fig. 8(a), gives the following contribution to $(\delta \mathcal{L})_{\text{first}}$,

$$\sum_{1,2,3} G(\vec{e}_{1;23}) \langle \vec{0} | \delta L | \bar{1}; 23 \rangle \langle \bar{1}; 23 | \delta L | \vec{0} \rangle \rho(J) , \quad \text{where} \quad G(\vec{e}_{1;23}) = \frac{1}{\omega_{p_1; p_2, p_3} + i\epsilon} , \quad (\text{A.12})$$

which, upon evaluating, gives,

$$\frac{1}{4} \sum_{1,2,3} |\lambda_{123}|^2 \frac{1}{\omega_{p_1; p_2, p_3} + i\epsilon} (\partial_1 - \partial_2 - \partial_3) J_1 J_2 J_3 (\partial_2 + \partial_3 - \partial_1) \rho(J) , \quad (\text{A.13})$$

where we made use of the commutator $[\partial, \sqrt{J}] = \frac{1}{2J} \sqrt{J}$. The second diagram is just the first diagram with arrows reversed, which gives the same contribution but with a denominator that has

an extra minus sign for $\omega_{p_1;p_2,p_3}$. Adding the two and using (A.5) we recover the leading order kinetic equation,

$$\frac{\partial n_a}{\partial t} = 2\pi \sum_{1,2,3} |\lambda_{123}|^2 (\delta_{1a} - \delta_{2a} - \delta_{3a}) \delta(\omega_{p_1;p_2,p_3}) \left(\frac{1}{n_1} - \frac{1}{n_2} - \frac{1}{n_3} \right) n_1 n_2 n_3 . \quad (\text{A.14})$$

Next-to-leading order

We now look at the terms that appear at next order. All terms in $(\delta\mathcal{L})_{\text{second}}$ (A.7), with two intermediate states vanish, so we look at $(\delta\mathcal{L})_{\text{third}}$, which has three intermediate states. One such

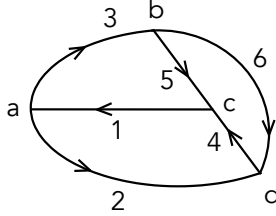


Figure 9: We start with the vacuum. The intermediate states are then $|\bar{1}; 23\rangle$, followed by $|\bar{1}; 256\rangle$, followed by $|\bar{4}; 26\rangle$, and ending in the vacuum.

sequence of intermediate states is shown in Fig 9. Evaluating the contribution of this diagram gives,

$$\begin{aligned} \delta\mathcal{L}_t(\{a, b, c, d\}) &= \sum_{1,\dots,6} \lambda_{123} \lambda_{426}^* \lambda_{356} \lambda_{145}^* G(\vec{e}_{1;23}) G(\vec{e}_{1;256}) G(\vec{e}_{4;26}) \\ &(\partial_1 - \partial_2 - \partial_3) J_1 J_2 J_3 (\partial_3 - \partial_5 - \partial_6) J_5 J_6 (\partial_4 + \partial_5 - \partial_1) J_4 (\partial_2 + \partial_6 - \partial_4) \rho(\vec{J}) . \quad (\text{A.15}) \end{aligned}$$

Using $\rho(\vec{J})$ (A.8) and evaluating the integral of $\delta\mathcal{L}_t(\{a, b, c, d\})$ multiplied by J_r , as prescribed by (A.5), gives,

$$\begin{aligned} \int dJ J_r \delta\mathcal{L}_t(\{a, b, c, d\}) &= \sum_{1,\dots,6} \lambda_{123} \lambda_{426}^* \lambda_{356} \lambda_{145}^* G(\vec{e}_{1;23}) G(\vec{e}_{1;256}) G(\vec{e}_{4;26}) \\ &(\delta_{1r} - \delta_{2r} - \delta_{3r}) \frac{1}{n_3} \left(\frac{1}{n_1} - \frac{1}{n_5} \right) \left(\frac{1}{n_2} + \frac{1}{n_6} - \frac{1}{n_4} \right) \prod_{i=1}^6 n_i . \quad (\text{A.16}) \end{aligned}$$

This matches the last term in (3.9). In more detail, in the main body of the text, the kinetic equation resulted by inserting contributions to the equal-time three-point function, such as (3.9), into (2.20). The contribution to the kinetic equation of the last term of (3.9) is what essentially matches (A.16). Notice that (2.20) has a factor of $(\delta_{kp_1} - \delta_{kp_2} - \delta_{kp_3})$ in front, which is just the factor of $(\delta_{1r} - \delta_{2r} - \delta_{3r})$ in (A.16) in slightly different notation.

There are other possible intermediate states. We can obtain them by changing the order in

which the vertices appear. For instance, the ordering a, d, c, b , shown below, gives the contribution,

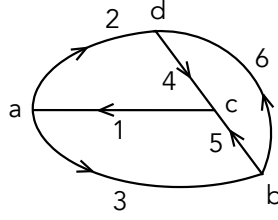


Figure 10: A different sequence of intermediate states: $|\bar{1}; 23\rangle$, followed by $|\bar{16}; 34\rangle$, followed by $|\bar{56}; 3\rangle$.

$$\delta\mathcal{L}_t(\{a, d, c, b\}) = \sum_{1, \dots, 6} \lambda_{123} \lambda_{426}^* \lambda_{356} \lambda_{145}^* G(\vec{e}_{1;23}) G(\vec{e}_{16;34}) G(\vec{e}_{56;3})$$

$$(\partial_1 - \partial_2 - \partial_3) J_1 J_2 J_3 (\partial_2 + \partial_6 - \partial_4) J_4 J_6 (\partial_4 + \partial_5 - \partial_1) J_5 (\partial_3 - \partial_5 - \partial_6) \rho(\vec{J}) . \quad (\text{A.17})$$

Of course, both these diagrams are simply redrawings of the tetrahedron diagram that appeared in Fig. 3. We need to consider all 24 permutations of the vertices. The six terms with vertex a first will give the six terms in (3.9). The six terms with vertex c first will give the same thing, but complex conjugated and with a relative minus sign. So their sum is just the imaginary part of the terms with vertex a first. We therefore reproduce the contribution of (3.9) to the kinetic equation (notice that (2.20) takes the imaginary part of the coupling multiplying the three-point function). The terms with vertex b first combined with the terms with vertex d first (which are the complex conjugate), reproduce the contribution of the tetrahedron in Fig. 3) with $5 \rightarrow -5$. We may do a similar analysis for the propagator renormalization diagram, but this is unnecessary, as we will now give a general argument that the results will always match what is in the main body of the text.

General Prescription

In implementing the perturbative solution of the Liouville equation, (A.3), we need to construct the sequences of all possible intermediate states. This can be represented by vacuum Feynman diagrams. Each Feynman diagram is topologically distinct. For each Feynman diagram we move around the vertices, so as to consider all possible orderings and correspondingly all possible intermediate states. Without loss of generality, we can pick one of the vertices to be first, while considering different orderings of the other vertices. If we cut the Feynman diagram at this first vertex, separating the edges entering it, then we have a diagram that contributes to a q -point correlation (for a q -body interaction). In particular, it may be a diagram for either a correlator such as $\langle a_1 a_2^\dagger a_2^\dagger \rangle$ (for $q = 3$), or its complex conjugate $\langle a_1^\dagger a_2 a_3 \rangle$. The complex conjugate arises if we reverse all the arrows on the Feynman diagram. We can account for this by including only

one Feynman diagram out of each pair that have all arrows reversed relative to each other and then taking the imaginary part, as we saw earlier. We can achieve this by drawing all diagrams contributing to $\langle a_1 a_2^\dagger a_2^\dagger \rangle$ (for $q = 3$) and connecting the external lines together to meet at a vertex. We then consider all possible orderings of the other vertices, which determines the intermediate states.

At this stage the number of terms we have matches what was discussed in Sec. 4. Now let us show that the terms are in fact the same. We get from vertex to vertex with a propagator $\frac{1}{-\vec{n}\cdot\vec{\omega}+i\epsilon}$, see (A.3), where $|\vec{n}\rangle$ is the current state. This matches the prescription given in Step 3 (4.1) of having a denominator with a sum of all incoming frequencies minus all outgoing frequencies. In our situation here the imaginary loop encloses all vertices visited so far. At each vertex we also have a transition matrix of δL , see (A.10) or (A.11). We see that it involves $(\partial_k + \partial_l + \dots - \partial_\alpha - \partial_\beta - \dots)$ where $\omega_k, \omega_l, \dots$ are the frequencies of the lines entering the vertex and $\omega_\alpha, \omega_\beta, \dots$ are the frequencies of the lines leaving the vertex. The transition matrix element also has factors of $\sqrt{J_i}$ and of n'_i/J_i , see (A.11). However, the latter can be eliminated by appropriately commuting through the $\sqrt{J_i}$. The end result, as seen in, for example, (A.15), is that one has each J_i appear once, immediately to the right of when the corresponding ∂_i appears. After inserting $\rho(J)$ that is an exponential, (A.8), it is clear we reproduce Steps 4 and 5 (4.2). Similar rules were found in [30, 31].

B. Symmetries

In this Appendix we show that the symmetries of the Hamiltonian, combined with the symmetries of the some of the Feynman diagrams, provide an efficient way of finding many of the contributions to the kinetic equation. We will, for instance, show that once one has any of the six terms appearing in the contribution of the tetrahedron diagram (3.9) the five others follow by a symmetry transformation.

Symmetries of the Hamiltonian

We first note the symmetries of the Hamiltonian, written in action-angle variables (A.9). The Hamiltonian is invariant under,

$$\omega_i \rightarrow -\omega_i, \quad J_i \rightarrow -J_i, \quad \alpha_i \rightarrow -\alpha_i, \quad \lambda_{123} \rightarrow -i\lambda_{-1-2-3} \equiv -i\lambda_{123}^*, \quad i = 1, 2, 3 \quad (\text{B.1})$$

Note that λ_{123}^* transforms in the same way, $\lambda_{123}^* \rightarrow -i\lambda_{123}$. The Hamiltonian is also invariant under a flip in sign of just two indices,

$$\omega_i \rightarrow -\omega_i, \quad J_i \rightarrow -J_i, \quad \alpha_i \rightarrow -\alpha_i, \quad \lambda_{123} \rightarrow \lambda_{-1-23} \equiv \lambda_{213}, \quad i = 1, 2 \quad (\text{B.2})$$

or a flip in one index,

$$\omega_2 \rightarrow -\omega_2, \quad J_2 \rightarrow -J_2, \quad \alpha_2 \rightarrow -\alpha_2, \quad \lambda_{123} \rightarrow -i\lambda_{1-23} \equiv -i\lambda_{321}^*, \dots \quad (\text{B.3})$$

This is useful because we sometimes have diagrams which have some arrows flipped relative to other diagrams. Flipping an arrow means flipping the sign of α . Due to the symmetries of the Hamiltonian we can instead flip the signs of the ω_{p_i} and J_i , and change the couplings, as stated above. Note that in the kinetic equation we have n_i instead of J_i (the former is the expectation value of the latter). So an arrow going in the opposite direction on line i means that in the contribution to the kinetic equation n_i , ω_{p_i} , and δ_{ir} all pick up a minus sign.

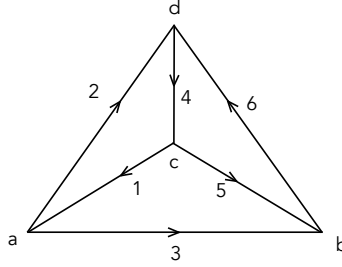


Figure 11: There is one tetrahedron diagram, which is related by symmetry to the tetrahedron diagram evaluated in Fig. 3.

We mentioned in the main body that, in addition to the tetrahedron diagram in Fig. 3 that we evaluated, there is another diagram, which is just Fig. 3 with the arrow on line 5 reversed, as shown in Fig. 11. In our new notation, $5 \rightarrow -5$. This means that its contribution is (3.9) with $n_5 \rightarrow -n_5$, $\omega_{p_5} \rightarrow -\omega_{p_5}$, and the couplings $\lambda_{356}^* \lambda_{145}$ replaced by $-\lambda_{635} \lambda_{451}^*$.

Symmetries of the diagrams

We will now show that the different contributions of a single tetrahedron diagram are related by symmetry as well.

Transformations of a tetrahedron

Let us look at the tetrahedron diagram studied in Sec. 3.2, and shown again below in Fig. 12(a), and consider all its symmetry transformation. There are 24 in total, corresponding to the 4! possible positionings of the vertices. The symmetry transformations that we use are rotations of the tetrahedron as well as mirror reflections. For instance, in Fig. 12 we have shown the 6 transformations that leave vertex a fixed: Fig. 12 (a) is the identity, Fig. 12 (b) is a rotation about vertex a , Fig. 12 (c) is a further rotation. Fig. 12 (d) is a mirror reflection of Fig. 12 (a) along the plane holding the 1 line fixed and bisecting the face bordered by lines 2, 3, 6. Fig. 12 (e) is a mirror reflection of Fig. 12 (b) holding the 2 line fixed, and Fig. 12 (f) is a mirror reflection of Fig. 12 (c)

holding the 3 line fixed. Fig. 12(a) has vertices labeled a, b, c, d and edges labelled 1, 2, 3, 4, 5, 6.

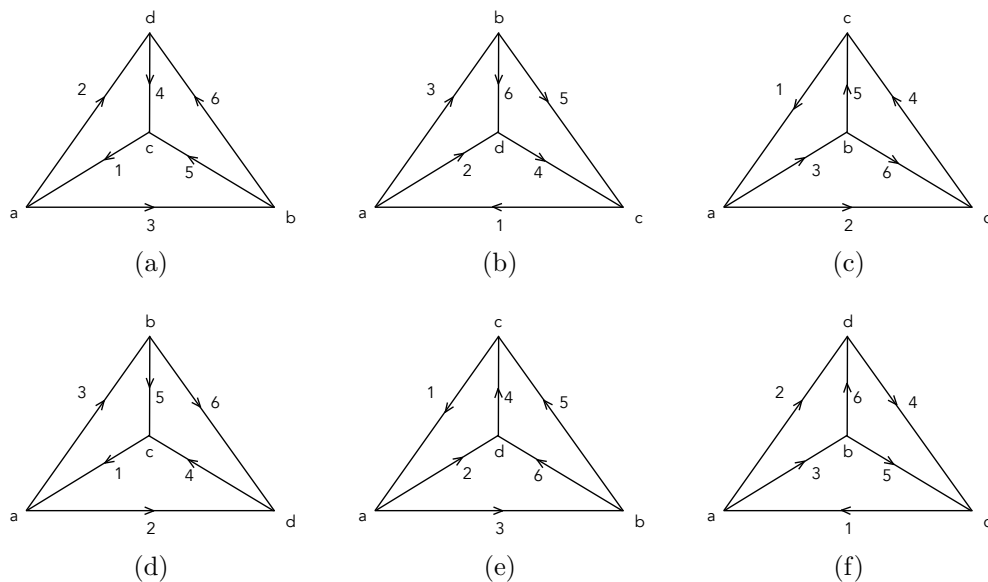


Figure 12: The vertex orderings of the tetrahedra are: a) a, b, c, d ; b) a, c, d, b ; c) a, d, b, c ; d) a, d, c, b ; e) a, b, d, c ; f) a, c, b, d .

This is recorded as the first entry in our table below. We see that, for instance, Fig. 12(e) has vertices a, b, d, c and edges $-2, -1, 3, -4, 6, 5$, where we are using a minus sign to denote the arrow running in the opposite direction. We have recorded this as the second entry in our table. The other entries are found in a similar manner.

vertex ordering	edges
a, b, c, d	1, 2, 3, 4, 5, 6
a, b, d, c	$-2, -1, 3, -4, 6, 5$
a, c, b, d	$-3, 2, -1, -6, -5, -4$
a, c, d, b	$-2, 3, -1, 6, -4, -5$
a, d, b, c	$-3, -1, 2, -5, -6, 4$
a, d, c, b	1, 3, 2, 5, 4, -6
b, a, c, d	$-5, 6, -3, 4, -1, 2$
b, a, d, c	$-6, 5, -3, -4, 2, -1$
b, c, a, d	3, 6, 5, $-2, 1, -4$
b, c, d, a	$-6, -3, 5, 2, -4, 1$
b, d, a, c	3, 5, 6, 1, $-2, 4$
b, d, c, a	$-5, -3, 6, -1, 4, -2$

vertex ordering	edges
c, a, b, d	5, $-4, 1, -6, 3, 2$
c, a, d, b	4, $-5, 1, 6, 2, 3$
c, b, a, d	$-1, -4, -5, -2, -3, 6$
c, b, d, a	4, 1, $-5, 2, 6, -3$
c, d, a, b	$-1, -5, -4, -3, -2, -6$
c, d, b, a	5, 1, $-4, 3, -6, -2$
d, a, b, c	6, 4, $-2, -5, 3, -1$
d, a, c, b	$-4, -6, -2, 5, -1, 3$
d, b, a, c	2, 4, $-6, 1, -3, 5$
d, b, c, a	$-4, -2, -6, -1, 5, -3$
d, c, a, b	2, $-6, 4, -3, 1, -5$
d, c, b, a	6, $-2, 4, 3, -5, 1$

Transforming terms in the kinetic equation

Let us now show how we can use these symmetries to relate different terms in the kinetic equation. In particular, we start with one of terms, (A.16), and define the right hand side of (A.16) without the couplings to be $t(a, b, c, d)$,

$$\begin{aligned} t(a, b, c, d) &= \tilde{t}(a, b, c, d) (\delta_{1r} - \delta_{2r} - \delta_{3r}) , \\ \tilde{t}(a, b, c, d) &= G(\vec{e}_{1;23})G(\vec{e}_{1;256})G(\vec{e}_{4;26})\frac{1}{n_3}\left(\frac{1}{n_1} - \frac{1}{n_5}\right)\left(\frac{1}{n_2} + \frac{1}{n_6} - \frac{1}{n_4}\right)\prod_{i=1}^6 n_i . \end{aligned} \quad (\text{B.4})$$

We view $t(a, b, c, d)$ as a function of the six edges, $t(1, 2, 3, 4, 5, 6)$. The contribution to the kinetic equation of the other terms will still be given by t , but the arguments will contain some permutation of these six variables, and they may have minus signs. For instance, consider the term in which we have swap vertices c and d , which by our table corresponds to,

$$\begin{aligned} t(a, b, d, c) &= t(-2, -1, 3, -4, 6, 5) \\ &= -(\delta_{1r} - \delta_{2r} - \delta_{3r}) G(\vec{e}_{1;23})G(\vec{e}_{1;256})G(\vec{e}_{1;45})\frac{1}{n_3}\left(\frac{-1}{n_2} - \frac{1}{n_6}\right)\left(\frac{-1}{n_1} + \frac{1}{n_5} + \frac{1}{n_4}\right)\prod_{i=1}^6 n_i . \end{aligned} \quad (\text{B.5})$$

Under this permutation, the couplings transform as

$$\lambda_{123}\lambda_{426}^*\lambda_{356}\lambda_{145}^* \rightarrow \lambda_{-2-13}\lambda_{-4-15}^*\lambda_{365}\lambda_{-2-46}^* = \lambda_{123}\lambda_{426}^*\lambda_{356}\lambda_{145}^* . \quad (\text{B.6})$$

We now collect all 6 terms that have vertex a first. We denote its contribution to the kinetic equation by,

$$\sum_{1, \dots, 6} \lambda_{123}\lambda_{426}^*\lambda_{356}\lambda_{145}^* (\delta_{1r} - \delta_{2r} - \delta_{3r}) T_a \quad (\text{B.7})$$

$$T_a = \tilde{t}(a, b, c, d) + \tilde{t}(a, b, d, c) - \tilde{t}(a, c, b, d) - \tilde{t}(a, c, d, b) - \tilde{t}(a, d, b, c) - \tilde{t}(a, d, c, b) .$$

The minus sign factors are due to the couplings picking up a minus sign. If we wish we can write this explicitly,

$$\begin{aligned} T_a &= G(\vec{e}_{1;23})\prod_{i=1}^6 n_i \left\{ \frac{1}{n_1} G(\vec{e}_{45;23}) \left[G(\vec{e}_{56;3}) \left(\frac{1}{n_4} - \frac{1}{n_2} \right) \left(\frac{1}{n_5} + \frac{1}{n_6} - \frac{1}{n_3} \right) + G(\vec{e}_{4;26}) \left(\frac{1}{n_5} - \frac{1}{n_3} \right) \left(\frac{1}{n_4} - \frac{1}{n_2} - \frac{1}{n_6} \right) \right] \right. \\ &\quad - \frac{1}{n_2} G(\vec{e}_{16;34}) \left[G(\vec{e}_{56;3}) \left(\frac{1}{n_1} - \frac{1}{n_4} \right) \left(\frac{1}{n_5} + \frac{1}{n_6} - \frac{1}{n_3} \right) + G(\vec{e}_{1;45}) \left(\frac{1}{n_6} - \frac{1}{n_3} \right) \left(\frac{1}{n_1} - \frac{1}{n_4} - \frac{1}{n_5} \right) \right] \\ &\quad \left. - \frac{1}{n_3} G(\vec{e}_{1;256}) \left[G(\vec{e}_{1;45}) \left(\frac{-1}{n_2} - \frac{1}{n_6} \right) \left(\frac{1}{n_1} - \frac{1}{n_4} - \frac{1}{n_5} \right) + G(\vec{e}_{4;26}) \left(\frac{1}{n_1} - \frac{1}{n_5} \right) \left(\frac{-1}{n_2} + \frac{1}{n_4} - \frac{1}{n_6} \right) \right] \right\} . \end{aligned} \quad (\text{B.8})$$

This of course is just (3.9). Now, the contribution of the terms with vertex c first is,

$$- \sum_{1, \dots, 6} \lambda_{123} \lambda_{426}^* \lambda_{356} \lambda_{145}^* (\delta_{1r} - \delta_{4r} - \delta_{5r}) T_c , \quad (\text{B.9})$$

where T_c can be related to T_a by a rotation of the tetrahedron that transforms vertex a into vertex c . There are multiple ways of doing this, which differ by permutations of the other three vertices. Picking the rotation $\{a, b, c, d\} \rightarrow \{c, d, a, b\}$, and using the corresponding entry in the table, we have,

$$T_c = T_a(-1, -5, -4, -3, -2, -6) = T_a(1, 5, 4, 3, 2, 6)^* , \quad (\text{B.10})$$

where in the second equality we used that flipping all the arrows corresponds to complex conjugating. Since under the change of variables $2, 3 \leftrightarrow 5, 4$, the product of couplings transforms into its complex conjugate, $\lambda_{123} \lambda_{426}^* \lambda_{356} \lambda_{145}^* \rightarrow \lambda_{123}^* \lambda_{426} \lambda_{356}^* \lambda_{145}$, the sum of the terms in which vertex a is first and vertex c is first is,

$$2i \operatorname{Im} \sum_{1, \dots, 6} (\delta_{1r} - \delta_{2r} - \delta_{3r}) \lambda_{123} \lambda_{426}^* \lambda_{356} \lambda_{145}^* T_a(1, 2, 3, 4, 5, 6) , \quad (\text{B.11})$$

as was stated earlier. Next, we look at the contribution of terms in which vertex b is first,

$$- \sum_{1, \dots, 6} \lambda_{123} \lambda_{426}^* \lambda_{356} \lambda_{145}^* (\delta_{3r} - \delta_{5r} - \delta_{6r}) T_b$$

$$T_b = \tilde{t}(b, a, c, d) + \tilde{t}(b, a, d, c) + \tilde{t}(b, c, a, d) + \tilde{t}(b, c, d, a) + \tilde{t}(b, d, a, c) + \tilde{t}(b, d, c, a) . \quad (\text{B.12})$$

There is no need to compute T_b , because it can be related in a simple way to T_a : we simply rotate vertex a into vertex b . There are multiple of doing this, which differ by permutations of the other three vertices. Picking the rotations $\{a, b, c, d\} \rightarrow \{b, d, a, c\}$, and using the corresponding entry in the table, we have,

$$T_b = T_a(3, 5, 6, 1, -2, 4) . \quad (\text{B.13})$$

Note the minus sign in front of (B.12) was placed there to account for minus sign acquired by the couplings under this transformation. Explicitly, T_b is,

$$T_b = G(\vec{e}_{3;56}) \prod_{i=1}^6 n_i \left\{ \frac{1}{n_3} G(\vec{e}_{1;256}) \left[G(\vec{e}_{4;26}) \left(\frac{1}{n_1} - \frac{1}{n_5} \right) \left(\frac{-1}{n_2} - \frac{1}{n_6} + \frac{1}{n_4} \right) + G(\vec{e}_{1;45}) \left(\frac{1}{n_2} + \frac{1}{n_6} \right) \left(\frac{1}{n_4} + \frac{1}{n_5} - \frac{1}{n_1} \right) \right] \right.$$

$$- \frac{1}{n_5} G(\vec{e}_{34;16}) \left[G(\vec{e}_{4;26}) \left(\frac{1}{n_1} - \frac{1}{n_3} \right) \left(\frac{1}{n_2} - \frac{1}{n_4} + \frac{1}{n_6} \right) + G(\vec{e}_{23;1}) \left(\frac{1}{n_6} - \frac{1}{n_4} \right) \left(\frac{1}{n_1} - \frac{1}{n_2} - \frac{1}{n_3} \right) \right]$$

$$\left. - \frac{1}{n_6} G(\vec{e}_{23;45}) \left[G(\vec{e}_{1;45}) \left(\frac{-1}{n_3} - \frac{1}{n_2} \right) \left(\frac{1}{n_4} + \frac{1}{n_5} - \frac{1}{n_1} \right) + G(\vec{e}_{23;1}) \left(\frac{1}{n_4} + \frac{1}{n_5} \right) \left(\frac{1}{n_1} - \frac{1}{n_2} - \frac{1}{n_3} \right) \right] \right\} . \quad (\text{B.14})$$

Finally, the contribution of terms with vertex d first is,

$$\sum_{1,\dots,6} \lambda_{123} \lambda_{426}^* \lambda_{356} \lambda_{145}^* (\delta_{4r} - \delta_{2r} - \delta_{6r}) T_d , \quad (\text{B.15})$$

where T_d is related to T_a by a rotation that transforms vertex a into vertex d . We pick the rotation $\{a, b, c, d\} \rightarrow \{d, b, c, a\}$, and using the corresponding entry in the table to get

$$T_d = T_a(-4, -2, -6, -1, 5, -3) = T_a(4, 2, 6, 1, -5, 3)^* = T_b(1, 5, 4, 3, 2, 6)^* . \quad (\text{B.16})$$

To summarize we have shown that all contributions to the kinetic equation from the tetrahedron diagrams are symmetry transformations of one of the terms, such as (B.4).

C. Manipulating the kinetic equation

In the main body of the text we found that the contribution of the tetrahedron diagram to the kinetic equation is,

$$2i \operatorname{Im} \sum_{1,\dots,6} (\delta_{1r} - \delta_{2r} - \delta_{3r}) \left[\lambda_{123} \lambda_{426}^* \lambda_{356} \lambda_{145}^* T_a(1, 2, 3, 4, 5, 6) - \lambda_{123} \lambda_{426}^* \lambda_{635}^* \lambda_{451} T_a(1, 2, 3, 4, -5, 6) \right] \quad (\text{C.1})$$

where T_a was given in (B.8) or equivalently the complex conjugate of (3.9). The second term is the tetrahedron diagram in Fig. 3 with the arrow on line 5 reversed, as discussed in Appendix B. This form of the kinetic equation is acceptable, but the form of the answer that has a more clear physical interpretation is one in which there are explicit delta functions. In particular, we write,

$$\frac{1}{\omega_{p_1;p_2p_3} + i\epsilon} = \frac{1}{\omega_{p_1;p_2p_3}} - i\pi\delta(\omega_{p_1;p_2p_3}) , \quad (\text{C.2})$$

where the first term comes with an implicit principal value. Using this, we may group terms based on the number of delta functions. This is what we partially do in this appendix.

One consistency check for our kinetic equation is that the thermal state should be stationary. In other words, inserting $n_i = 1/\omega_{p_i}$ into (C.1) should give zero. This is not manifest for the piece of (C.1) that has no delta functions. We will rewrite (C.1) in a way that will make it manifest, by showing that there is no such piece.

Another way of writing (C.1) is as,

$$\sum_{1,\dots,6} \lambda_{123} \lambda_{426}^* \lambda_{356} \lambda_{145}^* \left[(\delta_{1r} - \delta_{2r} - \delta_{3r}) T_a - (\delta_{3r} - \delta_{5r} - \delta_{6r}) T_b - (\delta_{1r} - \delta_{4r} - \delta_{5r}) T_c + (\delta_{4r} - \delta_{2r} - \delta_{6r}) T_d \right] \quad (\text{C.3})$$

where T_b, T_c, T_d were defined in Appendix B. We may rewrite (C.3), grouping terms based on which

δ_{ir} they come with,

$$\sum_{1,\dots,6} \lambda_{123} \lambda_{426}^* \lambda_{356} \lambda_{145}^* \left[\delta_{1r} (T_a - T_c) - \delta_{2r} (T_a + T_d) - \delta_{3r} (T_a + T_b) + \delta_{4r} (T_c + T_d) + \delta_{5r} (T_b + T_c) + \delta_{6r} (T_b - T_d) \right] \quad (\text{C.4})$$

If we use (C.2) and look at the piece with no delta functions, we notice that each pair of parenthesis in (C.4) vanishes, as it should.

Let us manipulate this part of the kinetic equation some more. Noting that under the change of variables $2, 3 \leftrightarrow 5, 4$, the product of couplings transforms into its complex conjugate, $\lambda_{123} \lambda_{426}^* \lambda_{356} \lambda_{145}^* \rightarrow \lambda_{123}^* \lambda_{426} \lambda_{356}^* \lambda_{145}$, we may rewrite (C.4) as,

$$2i \text{Im} \sum_{1,\dots,6} \lambda_{123} \lambda_{426}^* \lambda_{356} \lambda_{145}^* \left[\delta_{1r} T_a - \delta_{2r} (T_a + T_d) - \delta_{3r} (T_a + T_b) + \delta_{6r} T_b \right]. \quad (\text{C.5})$$

Or, we may alternatively write it as,

$$2i \text{Im} \sum_{1,\dots,6} \lambda_{123} \lambda_{426}^* \lambda_{356} \lambda_{145}^* \left[(\delta_{1r} - \delta_{2r} - \delta_{3r}) T_a - (\delta_{3r} - \delta_{5r} - \delta_{6r}) T_b \right]. \quad (\text{C.6})$$

If we wish, we can do a change of variables $(1, 2, 3, 4, 5, 6) \rightarrow (4, 5, 1, 6, 2, 3)$ on the T_b term, so as to rotate the b vertex into the a vertex to the greatest extent possible (meaning some of the arrows will be reversed; but we can't flip arrows under a change of variables. This gives back (C.1). Note that from this perspective, the second term in (C.1) makes sense, because if we had done the transformation taking us from a, b, c, d to b, d, a, c then the edges would have gone from $1, 2, 3, 4, 5, 6$ to $3, 5, 6, 1, -2, 4$ (see the table in Appendix. B), which is almost our transformation in the reverse direction, but with a minus sign for 5.

One delta function

Next, we look at the piece of C.1 which has one delta function. We will see that we can write this contribution to the kinetic equation entirely in terms of the following two functions,

$$\begin{aligned} D_{123} &= \prod_{i=1}^6 n_i \left(\frac{1}{n_1} - \frac{1}{n_2} - \frac{1}{n_3} \right) \delta(\omega_{p_1;p_2p_3}) \\ &\quad \left[\frac{-1}{n_4 n_5} \frac{1}{\omega_{p_3;p_5p_6}} \frac{1}{\omega_{p_4;p_2p_6}} + \frac{1}{n_4 n_6} \frac{1}{\omega_{p_1;p_4p_5}} \frac{1}{\omega_{p_3;p_5p_6}} + \frac{1}{n_5 n_6} \frac{1}{\omega_{p_1;p_4p_5}} \frac{1}{\omega_{p_4;p_2p_6}} \right], \\ D_{1256} &= \prod_{i=1}^6 n_i \left(\frac{1}{n_1} + \frac{1}{n_2} - \frac{1}{n_5} - \frac{1}{n_6} \right) \delta(\omega_{p_1p_2;p_5p_6}) \frac{1}{n_1 n_6} \frac{1}{\omega_{p_1;p_2p_3}} \frac{1}{\omega_{p_3;p_5p_6}}. \end{aligned} \quad (\text{C.7})$$

Like with T_a , these are functions of $(1, 2, 3, 4, 5, 6)$. There are a few special vertex orderings we will want to consider. We write them, along with the corresponding edges. The two functions we

just wrote are viewed as being at the vertex, $A \equiv \{a, b, c, d\} = (1, 2, 3, 4, 5, 6)$. We will also need,

$$\begin{aligned} A' &\equiv \{a, d, c, b\} = (1, 3, 2, 5, 4, -6) , & B &\equiv \{b, d, a, c\} = (3, 5, 6, 1, -2, 4) \\ C &\equiv \{c, d, a, b\} = (-1, -5, -4, -3, -2, -6) , & D &\equiv \{d, b, c, a\} = (-4, -2, -6, -1, 5, -3) . \end{aligned} \quad (\text{C.8})$$

We find that the piece of T_a that has terms with only one delta function is,

$$T_a = [D_{123}(A) + D_{123}(B) - D_{123}(C) + D_{123}(D)] + [(D_{1256}(A) - D_{1256}(A') + D_{1256}(B))] . \quad (\text{C.9})$$

Next, note that $T_b = T_a(B)$, $T_c = T_a(C)$, $T_d = T_a(D)$, and so we find,

$$\begin{aligned} T_b &= [D_{123}(A) + D_{123}(B) + D_{123}(C) - D_{123}(D)] + [-D_{1256}(A) - D_{1256}(A') + D_{1256}(B)] \\ T_c &= [-D_{123}(A) + D_{123}(B) + D_{123}(C) + D_{123}(D)] + [-D_{1256}(A) + D_{1256}(A') + D_{1256}(B)] \\ T_d &= [D_{123}(A) - D_{123}(B) + D_{123}(C) + D_{123}(D)] + [D_{1256}(A) + D_{1256}(A') + D_{1256}(B)] \end{aligned} \quad (\text{C.10})$$

Inserting into (C.4), we get for the terms with D_{123} ,

$$\begin{aligned} 2 \sum_{1, \dots, 6} \lambda_{123} \lambda_{426}^* \lambda_{356} \lambda_{145}^* &\left[\delta_{1r} [D_{123}(A) - D_{123}(C)] - \delta_{2r} [D_{123}(A) + D_{123}(D)] - \delta_{3r} [D_{123}(A) + D_{123}(B)] \right. \\ &\left. + \delta_{4r} [D_{123}(C) + D_{123}(D)] + \delta_{5r} [D_{123}(B) + D_{123}(C)] + \delta_{6r} [D_{123}(B) - D_{123}(D)] \right] . \end{aligned} \quad (\text{C.11})$$

By the same manipulations as done in the beginning of this section, this is equal to

$$\begin{aligned} 4 \sum_{1, \dots, 6} (\delta_{1r} - \delta_{2r} - \delta_{3r}) &\left[\text{Re}(\lambda_{123} \lambda_{426}^* \lambda_{356} \lambda_{145}^*) D_{123}(1, 2, 3, 4, 5, 6) \right. \\ &\left. - \text{Re}(\lambda_{123} \lambda_{426}^* \lambda_{635}^* \lambda_{451}) D_{123}(1, 2, 3, 4, -5, 6) \right] . \end{aligned} \quad (\text{C.12})$$

Now, for the terms with D_{1256} , looking at their appearance in (C.4) upon inserting (C.9) and (C.10) we get,

$$\begin{aligned} 2 \sum_{1, \dots, 6} \lambda_{123} \lambda_{426}^* \lambda_{356} \lambda_{145}^* &\left[(\delta_{1r} - \delta_{2r} - \delta_{5r} - \delta_{6r}) D_{1256}(A) - (\delta_{2r} + \delta_{3r} - \delta_{4r} - \delta_{5r}) D_{1256}(B) \right. \\ &\left. - (\delta_{1r} + \delta_{6r} - \delta_{3r} - \delta_{4r}) D_{1256}(A') \right] \end{aligned} \quad (\text{C.13})$$

Note also that since $D_{1256}(1, 2, 3, 4, 5, 6)$ is invariant under $2, 3 \leftrightarrow 5, 4$ we can replace the couplings with their real part,

$$2 \sum_{1, \dots, 6} \text{Re}(\lambda_{123} \lambda_{426}^* \lambda_{356} \lambda_{145}^*) \left[(\delta_{1r} - \delta_{2r} - \delta_{5r} - \delta_{6r}) D_{1256}(A) - (\delta_{2r} + \delta_{3r} - \delta_{4r} - \delta_{5r}) D_{1256}(B) - (\delta_{1r} + \delta_{6r} - \delta_{3r} - \delta_{4r}) D_{1256}(A') \right]. \quad (\text{C.14})$$

Finally, we rotate the B vertex and the A' vertex to the extent possible: for the term with $D_{1256}(B)$ we send $(1, 2, 3, 4, 5, 6) \rightarrow (4, 5, 1, 6, 2, 3)$, like we did after (C.6), and for the term with $D_{1256}(A')$ we send $(1, 2, 3, 4, 5, 6) \rightarrow (1, 3, 2, 5, 4, 6)$ and then do a change of variables $5 \leftrightarrow 6$. We get,

$$2 \sum_{1, \dots, 6} \left[\text{Re}(\lambda_{123} \lambda_{426}^* \lambda_{356} \lambda_{145}^*) (\delta_{1r} - \delta_{2r} - \delta_{5r} - \delta_{6r}) D_{1256}(1, 2, 3, 4, 5, 6) - (\delta_{1r} + \delta_{5r} - \delta_{2r} - \delta_{6r}) \left(\text{Re}(\lambda_{123} \lambda_{426}^* \lambda_{635}^* \lambda_{451}) D_{1256}(1, 2, 3, 4, -5, 6) + \text{Re}(\lambda_{123} \lambda_{146}^* \lambda_{635}^* \lambda_{245}) D_{1256}(1, 2, 3, 4, 6, -5) \right) \right] \quad (\text{C.15})$$

To summarize: we have taken the part of the kinetic equation due to the tetrahedron diagrams and extracted and simplified the piece that has one delta function. The result is the sum of (C.12) and (C.15).

One can continue, and extract the piece of the kinetic equation that has a product of two delta functions, and the piece that has a product of three delta functions. As we go to higher order in the nonlinearity, the kinetic equation will have products of an increasing number of delta functions. It would be useful to have a general prescription for extracting the coefficients of these delta functions. This would be a kind of extension of the cutting rules in finite temperature field theory, see e.g. [32].

D. Contact terms and lollipop diagrams

In this appendix, we provide justification for disregarding the square of the absolute value of $\frac{\delta H_{\text{int}}}{\delta a_k}$ in the interaction Lagrangian (2.11) (redundant interaction). Furthermore, we demonstrate that the existence of a non-zero expectation value for the complex field a_p in the cubic theory (2.3) does not affect our findings. We begin by addressing the redundant interaction.

Let us consider an expectation value of an operator $\mathcal{O}(a)$ constructed from the fields a_k and a_k^* . The m th order correction can be expressed as follows

$$\langle \mathcal{O}(a) \rangle^{(m)} = \left\langle \mathcal{O}(a) \frac{(-1)^m}{m!} \left(\int dt \sum_k \frac{1}{2\gamma_k n_k} \left[-i \mathcal{D}_k a_k \frac{\delta H_{\text{int}}}{\delta a_k} + \text{c.c.} \right] \right)^m \right\rangle + \dots, \quad \mathcal{D}_k = \partial_t + i\omega_k + \gamma_k. \quad (\text{D.1})$$

The first term on the right-hand side is obtained by expanding the path integral to the m th order in the interaction displayed in (2.11). The ellipsis represent terms involving the square of the

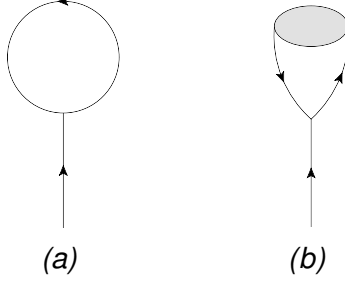


Figure 13: (a) A one-loop diagram contributing to $\langle a_p \rangle$ (b) Higher order corrections to $\langle a_p \rangle$. The gray blob represents corrections to the propagator of $\langle a_p^*(t)a_p(0) \rangle$.

absolute value of $\frac{\delta H_{\text{int}}}{\delta a_k}$, which we have omitted in (2.11). Now let us consider a specific set of terms that arises from pairing $\mathcal{D}_k a_k$ with $\mathcal{D}_k^* a_k^*$ in the first term of the above expression. This yields the following,

$$\begin{aligned} \langle \mathcal{O}(a) \rangle^{(m)} &= 2 \frac{m(m-1)}{2} \int dt_1 \int dt_2 \sum_k \frac{1}{4\gamma_k^2 n_k^2} \langle \mathcal{D}_k^* a_k^*(t_1) \mathcal{D}_k a_k(t_2) \rangle \\ &\times \left\langle \mathcal{O}(a) \frac{\delta H_{\text{int}}(t_1)}{\delta a_k^*} \frac{\delta H_{\text{int}}(t_2)}{\delta a_k} \frac{(-1)^m}{m!} \left(\int dt \sum_k \frac{1}{2\gamma_k n_k} \left[-i \mathcal{D}_k a_k \frac{\delta H_{\text{int}}}{\delta a_k} + \text{c.c.} \right] \right)^{m-2} \right\rangle + \dots, \end{aligned} \quad (\text{D.2})$$

where the overall constant represents a combinatorial factor that takes into account the possible number of pairings. Substituting

$$\langle \mathcal{D}_k^* a_k^*(t_1) \mathcal{D}_k a_k(t_2) \rangle = 2\gamma_k n_k \delta(t_1 - t_2), \quad (\text{D.3})$$

gives

$$\begin{aligned} \langle \mathcal{O}(a) \rangle^{(m)} &= \\ &\times \left\langle \mathcal{O}(a) \int dt_1 \sum_k \frac{1}{2\gamma_k n_k} \left| \frac{\delta H_{\text{int}}(t_1)}{\delta a_k^*} \right|^2 \frac{(-1)^{m-2}}{(m-2)!} \left(\int dt \sum_k \frac{1}{2\gamma_k n_k} \left[-i \mathcal{D}_k a_k \frac{\delta H_{\text{int}}}{\delta a_k} + \text{c.c.} \right] \right)^{m-2} \right\rangle + \dots. \end{aligned} \quad (\text{D.4})$$

Up to a sign, this expression is equal to the m th order term obtained by using $m-2$ interactions of the form shown in (2.11) and one interaction involving the square of the absolute value of $\frac{\delta H_{\text{int}}}{\delta a_k}$. Hence, these terms mutually cancel each other. Extending this conclusion to any number of pairings between $\mathcal{D}_k a_k$ and $\mathcal{D}_k^* a_k^*$ in (D.1), we can disregard the square of the absolute value of $\frac{\delta H_{\text{int}}}{\delta a_k}$ in the interaction Lagrangian L_{int} , as well as all diagrams resulting from pairing $\mathcal{D}_k a_k$ with $\mathcal{D}_k^* a_k^*$.

Next, we show how to get rid of the expectation value of the complex field a_p in the cubic theory (2.3). To leading order $\langle a_p \rangle$ is given by the lollipop diagram in Fig. 13(a). This diagram

can be evaluated using the Feynman rules in the main body of the text,

$$\langle a_p \rangle = \frac{-1}{\omega_p - i\gamma_p} \sum_k \lambda_{kpk}^* n_k + \mathcal{O}(\lambda^3) . \quad (\text{D.5})$$

Therefore, considering the momentum-conserving delta function in $\lambda_{p_1 p_2 p_3}$, we find that $\langle a_p \rangle$ is proportional to the Dirac delta function $\delta(\vec{p})$. It represents a shift from the zero value of the homogeneous background that defines the lowest energy state of the waves. The objective of our work is to study excitations around a constant background. To isolate degrees of freedom associated with excitations, we introduce the following *canonical* change of variables.

$$a_p \rightarrow a_p + b_0 \delta(\vec{p}) , \quad a_p^\dagger \rightarrow a_p^\dagger + b_0^* \delta(\vec{p}) , \quad (\text{D.6})$$

where the complex constant b_0 is defined by $\langle a_p \rangle = b_0 \delta(\vec{p})$; it can be calculated by evaluating the diagrams in Fig. 13(b). By definition, the expectation value of the shifted fields vanishes, and the Hamiltonian (2.3) takes the form

$$\begin{aligned} H \rightarrow & \sum_p \omega_p a_p^\dagger a_p + \frac{1}{2} \sum_{p_i} \left(\lambda_{p_1 p_2 p_3} a_{p_1}^\dagger a_{p_2} a_{p_3} + \lambda_{p_1 p_2 p_3}^* a_{p_1} a_{p_2}^\dagger a_{p_3} \right) + J_0 a_0^\dagger + J_0^* a_0 \\ & + \frac{1}{2} \sum_{p_1, p_2} \left(b_0^* \lambda_{0 p_1 p_2} a_{p_1} a_{p_2} + b_0 \lambda_{0 p_1 p_2}^* a_{p_1}^\dagger a_{p_2}^\dagger + 2b_0 \lambda_{p_1 p_2 0} a_{p_1}^\dagger a_{p_2} + 2b_0^* \lambda_{p_1 p_2 0}^* a_{p_1} a_{p_2}^\dagger \right) , \quad (\text{D.7}) \end{aligned}$$

where $J_0 = b_0 \omega_0 + |b_0|^2 \sum_p \lambda_{00p}^* + \frac{1}{2} b_0^2 \sum_p \lambda_{p00}$, and we have dropped the field independent constants (we have renormalized the cosmological constant). Due to the momentum-conserving delta function in $\lambda_{p_1 p_2 p_3}$, one can cancel the last two terms in the second line by suitably redefining ω_p (frequency renormalization),

$$\omega_p \rightarrow \omega_p - \sum_{p_2} (b_0 \lambda_{p p_2 0} + b_0^* \lambda_{p p_2 0}^*) . \quad (\text{D.8})$$

Thus, we obtain

$$\begin{aligned} H \rightarrow & \sum_p \omega_p a_p^\dagger a_p + \frac{1}{2} \sum_{p_1, p_2} \left(b_0^* \lambda_{0 p_1 p_2} a_{p_1} a_{p_2} + b_0 \lambda_{0 p_1 p_2}^* a_{p_1}^\dagger a_{p_2}^\dagger \right) \\ & + \frac{1}{2} \sum_{p_i} \left(\lambda_{p_1 p_2 p_3} a_{p_1}^\dagger a_{p_2} a_{p_3} + \lambda_{p_1 p_2 p_3}^* a_{p_1} a_{p_2}^\dagger a_{p_3} \right) + J_0 a_0^\dagger + J_0^* a_0 . \quad (\text{D.9}) \end{aligned}$$

To simplify this expression further, we employ a redefinition of the frequency as $\omega_p \rightarrow \mathcal{N}_p \omega_p$, along

with a corresponding field redefinition given by

$$\begin{aligned} a_p &\rightarrow \mathcal{N}_p^{-1/2} \left(a_p - \frac{1}{2\omega_p} \sum_{p_2} b_0 \lambda_{0pp_2}^* a_{p_2}^\dagger \right), & \mathcal{N}_p &= 1 - \frac{|b_0|^2}{4\omega_p^2} \sum_k |\lambda_{0pk}|^2, \\ a_p^\dagger &\rightarrow \mathcal{N}_p^{-1/2} \left(a_p^\dagger - \frac{1}{2\omega_p} \sum_{p_2} b_0^* \lambda_{0pp_2} a_{p_2} \right). \end{aligned} \quad (\text{D.10})$$

This transformation is canonical. As a result, up to linear terms in the fields, the Hamiltonian takes the original form (2.3)

$$H = \sum_p \tilde{\omega}_p a_p^\dagger a_p + \frac{1}{2} \sum_{p_i} \left(\tilde{\lambda}_{p_1 p_2 p_3} a_{p_1}^\dagger a_{p_2} a_{p_3} + \tilde{\lambda}_{p_1 p_2 p_3}^* a_{p_1} a_{p_2}^\dagger a_{p_3}^\dagger \right) + \tilde{J}_0 a_0^\dagger + \tilde{J}_0^* a_0, \quad (\text{D.11})$$

where quantities with tilde absorb various terms which emerge due to the field redefinition (D.10).⁹ By construction, the last two terms guarantee that $\langle a_0 \rangle = 0$.

We have shown that the expectation value of a_p in the cubic theory can be ignored by appropriately redefining the frequencies, couplings, and fields. To achieve this, one introduces a linear term of the form $J_0 a_0^\dagger + J_0^* a_0$ in the Hamiltonian (2.3), where the unspecified complex constant J_0 is appropriately tuned such that $\langle a_p \rangle = 0$ to all orders of the perturbative expansion. In other words, we can safely disregard the lollipop diagrams in Fig. 13. The value of $\langle a_p \rangle$ is determined by minimizing the complete effective potential of the model, whereas the Hamiltonian (2.3) describes only excitations.

References

- [1] K. Kawasaki and I. Oppenheim, “Logarithmic term in the density expansion of transport coefficients,” *Phys. Rev.* **139** (Sep, 1965) A1763–A1768.
- [2] J. R. Dorfman and E. G. D. Cohen, “Velocity correlation functions in two and three dimensions,” *Phys. Rev. Lett.* **25** (Nov, 1970) 1257–1260.
- [3] J. R. Dorfman, T. R. Kirkpatrick, and J. V. Sengers, “Why Non-equilibrium is Different,” [arXiv:1512.02679](https://arxiv.org/abs/1512.02679) [cond-mat.stat-mech].
- [4] J. R. Dorfman, H. van Beijeren, and T. R. Kirkpatrick, *Contemporary Kinetic Theory of Matter*. Cambridge University Press, 2021.
- [5] M. S. Green, “Boltzmann equation from the statistical mechanical point of view,” *The Journal of Chemical Physics* **25** (1956) no. 5, 836–855.

⁹It should be noted that cubic interactions of the form $a_{p_2} a_{p_2} a_{p_3}$ and $a_{p_1}^\dagger a_{p_2}^\dagger a_{p_3}^\dagger$ can also be eliminated through an appropriate field redefinition [13]. Consequently, we have omitted these terms in the final expression.

- [6] E. Cohen, “On the generalization of the boltzmann equation to general order in the density,” *Physica* **28** (1962) no. 10, 1025–1044.
- [7] R. Zwanzig, “Method for finding the density expansion of transport coefficients of gases,” *Physical Review* **129** (1963) no. 1, 486.
- [8] N. Bogoliubov, *Problems of Dynamic Theory in Statistical Physics*, 1946 .
- [9] J. Brocas, “On the comparison between two generalized boltzmann equations,” *Advances in Chemical Physics* (1967) 317–381.
- [10] R. Balescu, “Irreversible processes in ionized gases,” *The Physics of Fluids* **3** (1960) no. 1, 52–63.
- [11] I. Prigogine, *Non-equilibrium Statistical Mechanics*. Interscience Publishers, 1962. Reprint: Dover Publications, 2017.
- [12] R. Peierls, “On the kinetic theory of heat conduction in crystals,” *Ann. Phys.* **395** (1929) no. 8, 1055.
- [13] V. E. Zakharov, V. S. L’vov, and G. Falkovich, *Kolmogorov Spectra of Turbulence I: Wave Turbulence*. Springer-Verlag, 1992.
- [14] V. Zakharov, “Weak turbulence in media with a decay spectrum,” *J Appl Mech Tech Phys* **6** (1965) 22–24.
- [15] E. Falcon and N. Mordant, “Experiments in Surface Gravity – Capillary Wave Turbulence,” *Annual Review of Fluid Mechanics* **54** (Jan, 2022) 1–25, [arXiv:2107.04015](https://arxiv.org/abs/2107.04015) [physics.flu-dyn].
- [16] K. Hasselmann, “On the non-linear energy transfer in a gravity-wave spectrum part 1. general theory,” *Journal of Fluid Mechanics* **12** (1962) no. 4, 481–500.
- [17] A. I. Dyachenko, A. O. Korotkevich, and V. E. Zakharov, “Weak turbulence of gravity waves,” *Journal of Experimental and Theoretical Physics Letters* **77** (May, 2003) 546–550, [arXiv:0308101](https://arxiv.org/abs/0308101) [physics.flu-dyn].
- [18] V. Rosenhaus and M. Smolkin, “Feynman rules for forced wave turbulence,” *JHEP* **01** (2023) 142, [arXiv:2203.08168](https://arxiv.org/abs/2203.08168) [cond-mat.stat-mech].
- [19] V. Rosenhaus and G. Falkovich, “Interaction renormalization and validity of kinetic equations for turbulent states,” [[arXiv:2308.00033](https://arxiv.org/abs/2308.00033)] [hep-th].

- [20] V. Rosenhaus and M. Smolkin, “Wave turbulence and the kinetic equation beyond leading order,” [arXiv:2212.02555](https://arxiv.org/abs/2212.02555) [`cond-mat.stat-mech`].
- [21] X. Y. Hu and V. Rosenhaus, *in progress*.
- [22] P. B. Arnold, G. D. Moore and L. G. Yaffe, “Effective kinetic theory for high temperature gauge theories,” *JHEP* **01**, 030 (2003) doi:10.1088/1126-6708/2003/01/030, [arXiv:0209353](https://arxiv.org/abs/0209353) [`hep-ph`].
- [23] R. Micha and I. I. Tkachev, “Turbulent thermalization,” *Phys. Rev. D* **70** (2004) 043538, [arXiv:hep-ph/0403101](https://arxiv.org/abs/hep-ph/0403101).
- [24] P. B. Arnold and G. D. Moore, “The Turbulent spectrum created by non-Abelian plasma instabilities,” *Phys. Rev. D* **73** (2006) 025013, [arXiv:0509226](https://arxiv.org/abs/0509226) [`hep-ph`].
- [25] J. Berges, K. Boguslavski, S. Schlichting, and R. Venugopalan, “Turbulent thermalization process in heavy-ion collisions at ultrarelativistic energies,” *Phys. Rev. D* **89** no. 7, (2014) 074011, [arXiv:1303.5650](https://arxiv.org/abs/1303.5650) [`hep-ph`].
- [26] S. Schlichting and D. Teaney, “The First fm/c of Heavy-Ion Collisions,” *Ann. Rev. Nucl. Part. Sci.* **69** (2019) 447–476, [arXiv:1908.02113](https://arxiv.org/abs/1908.02113) [`nucl-th`].
- [27] D. Schubring, “Fokker-Planck approach to wave turbulence,” [arXiv:2309.08484](https://arxiv.org/abs/2309.08484) [`cond-mat.stat-mech`].
- [28] H. Wyld, “Formulation of the theory of turbulence in an incompressible fluid,” *Annals of Physics* **14** (1961) 143–165.
- [29] V. E. Zakharov and V. S. Lvov, “The statistical description of nonlinear wave fields,” *Radiophysics and Quantum Electronics* **18** (1975) no. 10, 1470–1487. <https://link.springer.com/content/pdf/10.1007/BF01040337.pdf>.
- [30] V. Gurarie, “Probability density, diagrammatic technique, and epsilon expansion in the theory of wave turbulence,” *Nucl. Phys. B* **441** (1995) 569–594, [arXiv:hep-th/9405077](https://arxiv.org/abs/hep-th/9405077).
- [31] A. Polyakov *unpublished*
- [32] P. F. Bedaque, A. K. Das, and S. Naik, “Cutting rules at finite temperature,” *Mod. Phys. Lett. A* **12** (1997) 2481–2496, [arXiv:hep-ph/9603325](https://arxiv.org/abs/hep-ph/9603325).